chemosensors

MDPI

Review

Recent Advances in Magnetic Nanoparticles-Assisted Microfluidic Bioanalysis

Zihui Zhong [1], Jincan He [1], Gongke Li [2] and Ling Xia [2,*]

[1] College of Public Health, Guangdong Pharmaceutical University, Guangzhou 510310, China
[2] School of Chemistry, Sun Yat-sen University, Guangzhou 510006, China
* Correspondence: xialing@mail.sysu.edu.cn; Tel.: +86-20-39339782

Abstract: Magnetic nanoparticles (MNPs) are attracting increasing attention in bioanalysis, due to their large surface area and excellent steerable properties. Meanwhile, the booming development of microfluidics is offering a faster, lower consumption, and more effective approach to bioanalysis. MNPs-assisted microfluidic bioanalysis enables enhanced analytical performance by introducing functionalized magnetic nanomaterial into microchip devices. This work reviews the advances of MNPs-assisted microfluidic bioanalysis in the recent decade. The preparation and modification methods of MNPs are summarized as having a bioanalysis capability in microchips. These MNPs can be used for sample pretreatment materials and/or biosensing tags. In sample pretreatment, MNPs enable effective magnetic separation, preconcentration, and mass transport. In detection, MNPs act as not only magnetic sensing tags but also as the support for optical sensors. Finally, the overviews and challenges in microfluidic bioanalysis with the assistance of MNPs are discussed.

Keywords: magnetic nanoparticles; microfluidics; sample pretreatment; biosensing; review

Citation: Zhong, Z.; He, J.; Li, G.; Xia, L. Recent Advances in Magnetic Nanoparticles-Assisted Microfluidic Bioanalysis. *Chemosensors* **2023**, *11*, 173. https://doi.org/10.3390/chemosensors11030173

Academic Editors: Lorena Gonzalez-Legarreta and David González-Alonso

Received: 16 January 2023
Revised: 27 February 2023
Accepted: 1 March 2023
Published: 3 March 2023

1. Introduction

Microfluidics capable of microscale fluid handling are thriving in powerful analytical technology, especially in biological analysis [1,2]. The miniaturized microfluidic chip device accelerates the mass transfer and heat exchange dramatically in the depth direction of channels [3]. Meanwhile, customized microchannel networks can be fabricated via microfabrication technology, which enables easy integration of analytical processes into a single microchip [4,5]. Armed to make analysis more cost-effective, microfluidics have received unprecedented development since the 1990s. However, in practical applications, microfluidics still suffers from complexity in both device fabrication and precision manipulation [6].

In the last decade, magnetic nanoparticles (MNPs) are attracting increasing attention in bioanalysis, due to their modifiable surface area and excellent steerable properties [7–9]. The introduction of MNPs into microfluidic bioanalysis not only can enlarge the application scope of microfluidics but also simplify the operation by applying an external magnet [10,11]. The publications and citations on MNPs in microfluidics are represented in Figure 1, revealing the increasing attention on these research fields in the last decade. In this review, an overview of the advances of MNPs-assisted microfluidic bioanalysis is carried out based on more than 200 references (Figure 2). The preparation and modification methods of MNPs are summarized as having bioanalysis capability in microchips. These MNPs can be used as sample pretreatment materials and/or biosensing tags. In sample pretreatment, MNPs enable effective magnetic separation, preconcentration, and mass transport. In detection, MNPs act as not only magnetic sensing tags but also as a support for optical sensors. Finally, the challenges in microfluidic bioanalysis with the assistance of MNPs are discussed.

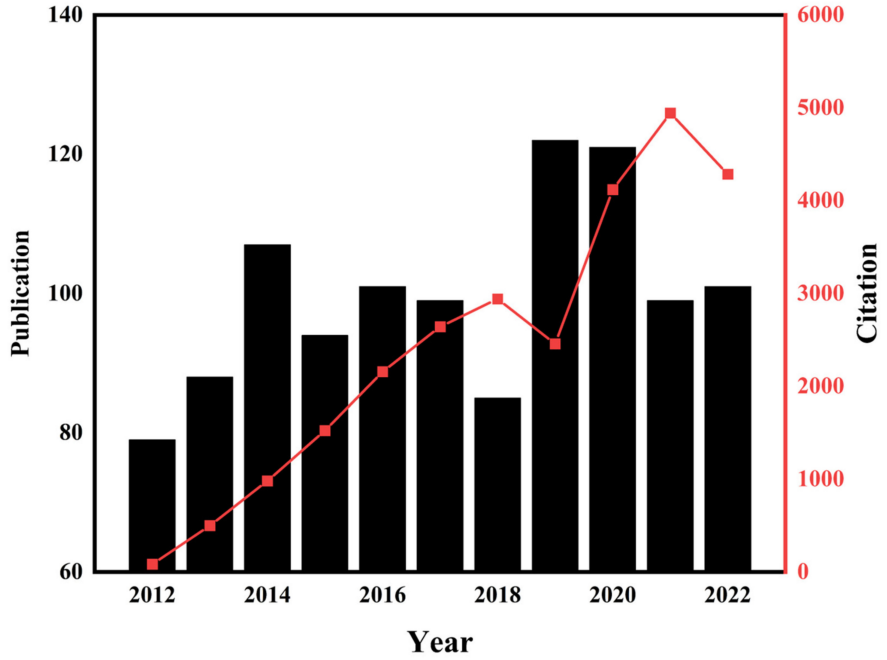

Figure 1. The steady increase of research on MNPs combined with microfluidics in total from 2012 to December 2022 (according to the web of science).

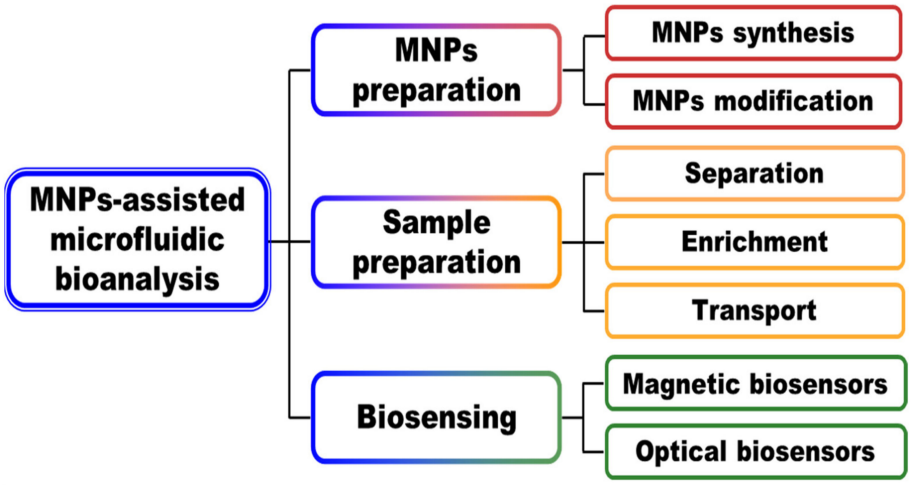

Figure 2. Schematic illustration of MNPs assisted-microfluidic bioanalysis.

2. Preparation and Modification of MNPs

2.1. Preparation of MNPs

The superparamagnetic character of MNPs utilized in microfluidic bioassay comes from metal-based magnetic materials, such as Fe_3O_4 or Fe_2O_3. Nanoparticles with superparamagnetic properties are frequently called magnetic beads (MBs) or beads due to their spherical shape. Microfluidics refers to the manipulation of fluids at small scales (generally from 10^{-8} to 10^{-18} L) in narrow (10^{-6} to 10^{-8} m) chambers or channels. Owing to their nanoscale size, MNPs can freely flow through the microchannels and be easily confined in the microstructures, resulting in efficient trapping. The ideal MNPs applied to microfluidic chips should have high magnetic properties, sufficiently small size with narrow distribution, excellent dispersion, and high surface functionality. These properties can be achieved by optimizing the preparation process of MNPs. The currently reported methods for the synthesis of MNPs include co-precipitation, solvothermal, thermal de-

composition, high-temperature solution phase reaction, and chemical reduction. Table 1 displays the benefits and drawbacks of various techniques for preparing MNPs.

Table 1. MNPs preparation and modification methods: Advantages and disadvantages.

Methods		Advantages	Disadvantages	Ref.
Preparation methods	co-precipitation	simple reaction conditions; high yield.	tend to severe agglomeration.	[12]
	solvothermal	well-crystallized narrow size distribution	harsh reaction conditions high temperature	[13,14] [15,16]
	thermal decomposition high-temperature solution phase reaction	size control	high temperature; organic solvent required	[17]
	chemical reduction	paramagnetic, little particle agglomeration	high temperature	[18]
	commercial MBs	monodispersed; with functional groups	expensive; strong non-specific adsorption	[19–23]
Modification ways	coating with inorganic nanomaterials	excellent stability, reusable	complex preparation, reduced magnetic property	[24–29]
	modifying with organic materials	good dispersion, with functional groups	nonspecific adsorption	[30–38]
	coupling target ligands	selective identification	high requirements for preservation conditions	[39–48]

Fe^{3+} salt, divalent salts (such as Fe^{2+}, Ni^{2+}, Co^{2+}, and Mn^{2+}), and excess alkaline solution (e.g., ammonia or hydroxide solution) are all used in the co-precipitation synthesis process. For instance, Tamer et al. [12] were able to produce black Fe_3O_4 from $FeCl_3$ and $FeSO_4{\cdot}7H_2O$ after those raw materials were reacted with NaOH for 40 min. The formed MNPs carrying the analyte crossed the microchambers by using the simple magnet, which showed excellent magnetic properties. The co-precipitation method has advantages including simple reaction conditions and relatively high yield. However, the resulting MNPs trend to severe agglomeration, which is not favorable for application in microfluidic systems. A surfactant can be added or the pH value of the solution may be carefully adjusted to minimize the agglomeration.

The solvothermal method is performed in a sealed autoclave at an elevated temperature (130–250 °C), where an organic solvent is used as the reaction medium. For example, Cheng et al. [13] synthesized MNPs in an autoclave by the reaction of iron (III) chloride hexahydrate ($FeCl_3{\cdot}6H_2O$), sodium acetate (NaOAc), and ethylene glycol for 48 h at 200 °C. Hao et al. [14] prepared monodisperse Fe_3O_4 nanoparticles in a modified method by changing the reaction temperature and time to 100 °C and 10 h. These products were measured to be approximately 300 nm and showed no agglomeration, which could be well matched to the size of the microfluidic chip. The synthesis method can directly obtain well-crystallized MNPs but requires harsh reaction conditions.

MNPs can be synthesized via the thermal decomposition of organometallic precursors in an organic solvent with the assistance of a surfactant [15]. Lee et al. [16] reported that $MnFe_2O_4$ nanoparticles were prepared by thermal decomposition method using iron (III) acetylacetonate ($Fe(acac)_3$) and manganese (II) acetate ($Mn(ac)_2$) as precursors, oleic acid as ligand, trioctylamine as surfactant. The size of the nanoparticles was approximately 100 nm in diameter, and no aggregation phenomenon was found in many cases. The $MnFe_2O_4$ nanoparticles were applied to improve the performance of an immunoassay for detecting influenza infections by using an integrated microfluidic system. Thanks to the ability of surfactant to halt the nucleation process, this approach produces monodisperse MNPs that can be well applied to microfluidic systems.

For the synthesis of Fe_3O_4 and related MFe_2O_4 nanoparticles (with M = Co, Ni, Mn, Mg, etc.), metal acetylacetonates are heated up to 305 °C with a mixture of 1,2-hexadecane diol, oleic acid, and oleylamine. Chang et al. [17] reported that Fe_3O_4 MNPs were fabricated by the high-temperature solution phase reaction method as previously described. The size of nanoparticles can be well controlled by changing the reaction temperature or metal precursor in this method. Therefore, the problem of particle size matching between microfluidic chips and MNPs can be well solved.

The chemical reduction method usually involves the reduction of metal ions and in particular Fe^{2+} or Ni^{2+} by reducing agents such as sodium borohydride, hydrazine hydrate, and the addition of surfactants during the experiment to prepare MNPs. Li et al. [18] generated Ni/NiO nanoparticles by a chemical reduction reaction at a temperature of 400 °C. The nanoparticles synthesized by this method are paramagnetic, and the particle agglomeration can be reduced by the addition of surfactant. However, high temperature is required.

In addition, numerous magnetic-based products are commercially available to consumers, such as Dynabeads [19], Affimag SLC magnetic beads [20], Magnetic Activated Cell Sorting microbeads [21], Charge Switch® beads [22], and MagneSil® beads [23]. Dynabeads of the company Dynal Biotech (Waltham, MA, USA) are the source of magnetic separation technology. They are superparamagnetic nanoparticles with a polymer shell that are frequently employed in microfluidic systems because they are simple to modify with functional groups. The advantage of superparamagnetism is that they do not aggregate when the external magnetic field is removed or turned off, as there is no remaining permanent magnetization. This may be one of the key factors for their widespread application in microfluidic bioassays.

2.2. Modification of MNPs

In order to facilitate applications in bioanalysis, the surface chemistry of MNPs needs to be controlled. Usually, pristine MNPs tend to aggregate into large clusters due to their dipole-dipole interactions and large specific surface area, resulting in a decrease in their specific surface area and superparamagnetism. Therefore, surface modification of magnetic nanoparticles is required. Beyond magnetic steerable properties, surface modification endows MNPs with multiple functions, such as specific recognition or sensing. On the other hand, modified MNPs may prevent the nanoparticles from agglomeration when migrating in a microchannel, leading to colloidal stability. In addition, surface-modified MNPs can exhibit water solubility, biocompatibility, and the ability to avoid non-specific adsorption with biomolecules. Therefore, the surface-modified MNPs can be well combined with microfluidics and applied to bioanalysis. Figure 3 represents the most frequently used surface modification strategies, they are inorganic nanomaterials coating, organic materials modifying, and target ligands coupling.

The surface of MNPs can be coated with inorganic materials to produce magnetic nanocomplexes with a core-shell structure, which are more stable and easier to be modified. The most prevalent magnetic nanocomplexes are ferric oxide nanoparticles coated with silicon dioxide (Fe_3O_4@SiO_2). The silicon dioxide shell is coated to prevent antibodies and chemicals from interacting with the Fe_3O_4 core. This greatly reduces the non-specific adsorption of MNPs. The Fe_3O_4@SiO_2 nanoparticles had —CH(O)CH— or —COOH group on the surface, which not only enhance their biocompatibility and stability, but also made them accessible to crosslink with amino terminated antibodies [24], meta-iodobenzylguanidine and octreotide-2,2′,2″,2‴-(1,4,7,10-tetraazacyclododecane-1,4,7,10-tetrayl)tetraacetic acid labels [25], or polyethyleneimine [26]. In order to boost stability and make it easier for the target ligands to bind to the MNPs through metal-thiol interactions, precious metal nanomaterials were typically coated on the surface of MNPs as a shell. Fe_3O_4 nanoparticles were coated with Au nanoparticles to create Fe_3O_4@Au NPs (AuMPs), according to Gan et al. The magnetic aptamer probes formed by AuMPs nanoparticles and aptamer exhibited excellent stability and could be reused up to 20 times [27]. In addition, Stark et al. prepared carbon-coated nanomagnets having a core-shell structure, which possesses high air and thermal stability [28,29].

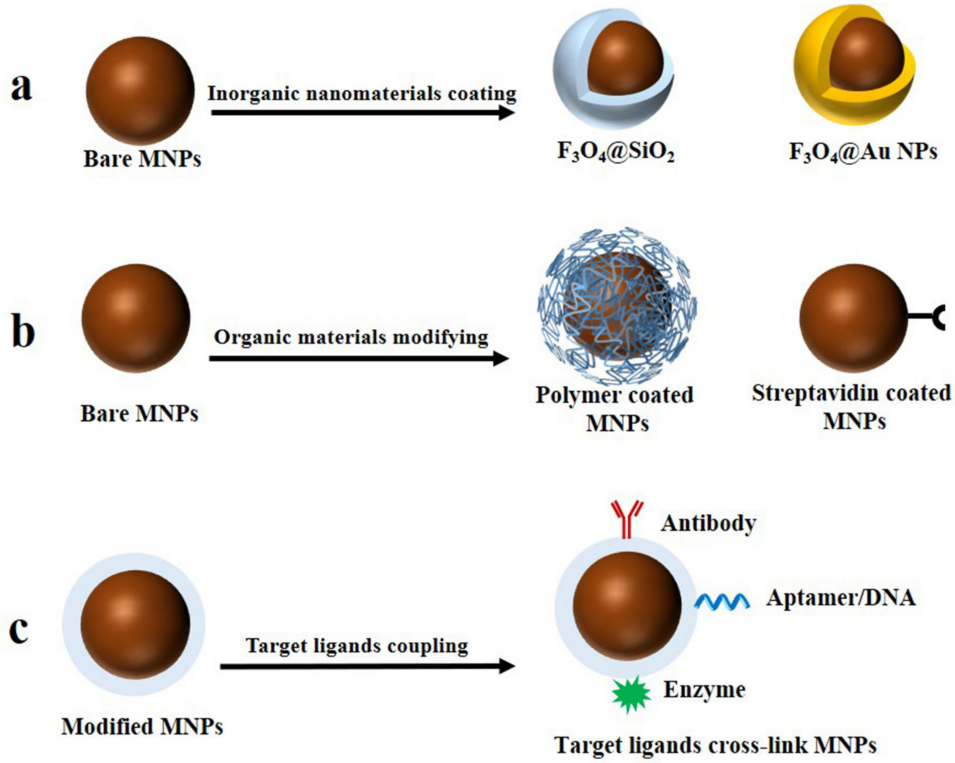

Figure 3. Strategies for MNPs modification. (**a**) Inorganic nanomaterials coating. (**b**) Organic materials modifying. (**c**) Target ligands coupling.

Surfactants or polymers are typically used in modifying the surfaces of MNPs. Tween-20 is a typical surfactant applied in research, the tween-20 and streptavidin-modified magnetic beads were reported by Jin et al. [30]. Tween-20 can effectively avoid beads aggregation and does not affect the antibody binding capacity of the beads. A good performance was also shown by the polymer-coated MNPs. Polyethylene glycol is an organic polymer, and it could be used to modify MNPs to enhance their water solubility and stability by adding functional groups such as amino [31]. In addition, polyethylene glycol-modified magnetic microspheres could reduce non-specific protein adsorption [32]. The MNPs modified by carboxyl-terminated polyacrylic acid exhibited excellent water solubility and dispersibility [33]. Very little non-specific adsorption occurred on the MNPs coated in polystyrene, and the reaction sites were activated. Specifically, the MNPs functionalized by molecularly imprinted polymers had particular bionic recognition characteristics [34]. Overall, the particles could be used directly for high loading binding to a wide range of biological ligands (proteins, peptides, oligonucleotides, drug molecules, etc.) [35].

Natural compounds can also modify the surface of MNPs. Chitosan is a perfect option for the capture and release of nucleic acids due to its free amino group composition. MNPs coated with chitosan made coupling of target ligands easier [36]. By specific binding of streptavidin-biotin, MBs coated with streptavidin could also capture avidin-labeled target ligands [37]. Owing to the tetrameric conformation of streptavidin, one streptavidin protein is able to bind four biotin molecules with high affinity and selectivity, which can improve the sensitivity of the assay. Notably, the RNA target capture efficiency of 4-formylbenzamide functionalized MBs was two orders of magnitude higher than the results of streptavidin-coated microbeads [38].

By further coupling target ligands, the surface-modified MNPs can significantly improve their selectivity in microfluidic bioassays. When coupling the MNPs to the target ligands, the coupling effectiveness could be increased by adding coupling agents that activate the carboxyl groups on the surface of the nanomaterials. N-(3-dimethylaminopropyl)-N′-ethylcarbodiimide hydrochloride (EDC) and N-hydroxy succinimide (NHS) [39] were the most frequently utilized coupling agents. Here, aminated DNA strands were conjugated with carboxylated MBs via a typical EDC/NHS coupling reaction [40]. Likewise, the quantum dots with carboxyl functional group were coupled to MBs with amine functional group by EDC/NHS cross-linking reaction [41]. When microfluidic chips are combined with MNPs to establish a test method for biochemical samples, there is a need to consider the selectivity of the assay for the testing target, in addition to overcoming the obstacles of particle size matching, particle deposition, and non-specific adsorption. Target ligands and in particular specifically and non-specifically recognized biomolecules are frequently employed to cross-link MNPs in microfluidic bioassay systems in order to improve the selectivity of the test method. Antibodies were the early biomolecules to be reported for specific recognition, usually coupled with MNPs as capture probes for target identification and separation, they exhibited good stability and high specificity [42]. Nucleic acid aptamers, which are commonly referred to as "artificial antibodies", can be synthesized by chemical methods that are simpler, faster, and cheaper. Lee et al. screened a "universal" aptamer that can predictably alter its conformation based on changes in solvent composition, enabling the detection of multiple viruses [43]. Additionally, methods for enriching exosomes based on antibody-antigen interactions were difficult to elute even under favorable conditions, which was harmful to subsequent analysis. Ye et al. [44,45] offered an analytical approach based on reversible affinity recognition between phosphatidylserine and Tim4 for magnetic enrichment and determination of exosomes on microarrays. Interestingly, dextran exhibited excellent potential for the isolation of influenza viruses, Lee et al. [46] were able to isolate influenza viruses based on the specificity of viral surface hemagglutinin antigen binding to dextran. In recent years, some non-specific biomolecules (such as mannose-binding lectin [47] and vancomycin [48]) had also been applied to modify MNPs to capture multiple bacteria simultaneously. Subsequently, sensitive and strain-specific detection of targeted bacteria could be achieved by using signal tag-labeled specific nucleotide probes.

3. MNPs in Microfluidic Bioanalysis

In microfluidic bioanalysis, functionalized MNPs by different preparation and surface modification methods can be introduced to boost the analytical performance in selectivity, sensitivity, and speed. In microfluidic sample preparation, MNPs assist the effective magnetic separation, preconcentration, and mass transport. Meanwhile, in bio-analyte detection, MNPs can be used as signal tags in magnetic response sensors or supporters for optical sensors.

3.1. MNPs-Assisted Microfluidic Sample Preparation

Aiming to separate and concentrate analytes from complex matrices, sample preparation before detection can improve the analytical results in selectivity, sensitivity, speed, and accuracy [49]. Surface-modified MNPs are utilized as magnetic carriers for the precise capture, separation, concentration, and transfer of analytes in the pretreatment unit of microfluidic bioanalytical systems.

3.1.1. Microfluidic Magnetic Separation

Surface modification, therefore, provides MNPs an edge over the other separation techniques (such as filtration, and centrifugation) that are time-consuming as well as laborious. For example, the coupling of biomolecules (such as antibodies, nucleic acid aptamers, antigens, enzymes, etc.) to MNPs has been used to achieve simple, fast, inexpensive, and highly efficient separation of targeted biomolecules under the effect of an external magnetic field. Common magnetic separation techniques include magnetic solid phase extraction, solid phase extraction, ion exchange separation, and chromatographic separation techniques.

MNPs are used as the sorbent in the dispersive solid-phase extraction method known as magnetic solid-phase extraction. Targeted analytes are introduced to the sample and bound to functionalized MNPs, then the analytes migrate with MNPs and dissociate from the sample matrix when an external magnetic field is applied. On a microfluidic chip, magnetic solid-phase extraction of analytes is carried out with simple operation, excellent separation efficiency, and minimal solvent consumption. DNA [50] and neutrophils [51] were successfully extracted using magnetic solid-phase extraction in microfluidic systems, with enhanced extraction yield and purity. The purified analytes could be further detected by off-line devices following magnetic solid-phase extraction, such as fluorescence immunoassay [52], chemiluminescence immunoassay [53], and ultraviolet absorption detection [54]. The analytical devices were integrated into the microfluidic system with instrument miniaturization and the development of integration technology, allowing for simultaneous separation and detection to meet the needs of the scenario for quick detection. Magnetic separation and direct immunoassay on chip were successfully used to separate and detect the hepatitis B virus [55] and breast cancer cells MCF-7 [56]. Compared with the direct method, the double antibody sandwich method is more specific. Zhang et al. [57] used MBs functionalized with capture antibodies to perform magnetic solid-phase extraction on MCF-7 cells, followed by imaging of the cells with fluorescein-labeled detection antibodies on microchips. The microfluidic device was capable of capturing circulating tumor cells from the blood with an efficiency higher than 94% and identifying MCF-7 cells. Using the same immunoassay, leukemia B cells were examined and eliminated [58]. In addition, the double antibody sandwich enzyme-linked immunoassay is the most traditional immunoassay technique. To increase the sensitivity of the analytical method, the captured antibody was modified on MBs rather than 96-well plates [59]. The large specific surface area of MBs can modify more captured antibodies and therefore, the sensitivity is greatly improved compared to the standard enzyme-linked immunosorbent assay. Furthermore, high-brightness quantum dots could take the place of the horseradish peroxidase enzyme, which eliminated the need for catalytic substrates and simplified the fluorescent immunoassay process with the detection limit of 4.45×10^5 particles/mL for exosomes of oral cancer origin [60]. Because of their tiny molecular weight, biological small molecules in particular nucleotide molecules have a restricted ability to be detected. Fluorescence immunoassay of *Helicobacter pylori* 16S rRNA [61], ovarian cancer's cell-free DNA [62], and the influenza virus RNA [63] was made possible by the addition of a polymerase chain reaction amplification module. It is worth noting that the proximity probe (which are oligonucleotide chains) immobilized MBs could also act as a signal label for fluorescence measurement when amplified by polymerase chain reaction besides being a capture probe. The point-of-care assay developed provides the merits of portability, less reagent consumption and faster time-to-results [64]. Simultaneous separation and detection are required since there are multiple subtypes of influenza A viruses [65]. To automatically isolate and detect multiple influenza hemagglutinin in early diagnosis, Liu et al. [66] made full use of MBs of various sizes and a fluorescent label called quantum dots. This assay realized high sensitivity with a detection limit of 4.5 ng/mL for H9N2 hemagglutinin and 3.4 ng/mL for H7N9 hemagglutinin. It is worth noting that the aqueous phase including reagents and biological sample was automatically flowed and reacted in the channel by a capillary pump on a chip after hydrophilic treatment of microfluidic channel surface. This eliminated the need for heavy pumps and avoided non-specific adsorption, which greatly reduced the device

size and improved the portability [67]. Various antibodies and enzymes can be used to functionalize individual MBs. To enable simultaneous detection of multiplexed biomarker proteins in clinical cancer diagnostics, the Rusling et al. [68] reported an ultra-sensitive electrochemical microfluidic array that used antibody-modified gold nanoparticles as a sensing array and antibody-modified MBs as probes for off-chip capture and separation of protein with a detection limit of less than 50 fg/mL (Figure 4a). In a follow-up study, for better application in clinical and point-of-care screening, the group integrated a protein capture chamber on a microfluidic chip to enable on-chip magnetic separation and detection of proteins [69]. Based on this, the researchers improved the immuno-array to further detect smaller peptide fragments. Detection limit of 150 amol/L were achieved for simultaneous determination of parathyroid hormone-related peptide isoforms and peptide fragments [70]. Without using a sandwich immunoassay and signal amplification strategy, Lima et al. [71] created a microfluidic method with an electrochemical capillary capacitor to achieve fast and sensitive detection of carbohydrate antigen 15-3, a biomarker protein for breast cancer, with a detection limit of 92.0 μU/mL. Incorporating on-chip magnetic separation technology with an electrochemical immunoassay based on enzyme amplification [72], the detection limit for myeloperoxidase was reached at 0.004 ng/mL. The detection limit of N-terminal prohormone brain natriuretic peptide by electrochemical immunoassay based on metal nanoparticle enhancement was 750.0 pmol/L [73]. Similar to this, the magnetic separation method and chemiluminescent immunoassay worked together to successfully isolate and identify single [74] or multiple analytes [75] on-chip. In recent years, surface enhanced Raman spectroscopy-based microfluidics has been a popular study area. After magnetic separation of the analyte, antibody-modified MBs created immune complexes with an antibody-modified Raman nanotag, the surface enhanced Raman signals of immune complexes were detected in the detection chamber, and the detection limit of prostate specific antigen was 0.01 ng/mL [76]. Notably, using the droplet microfluidic device for simultaneous detection of dual prostate antigens, the magnetic separation, washing and surface enhanced Raman spectroscopy detection were all carried out in sequential droplets, without any manual incubation and washing steps. The robustness of the surface enhanced Raman spectroscopy approach was increased by averaging Raman signals for continuous droplets, and the limits of detection were below 0.1 ng/mL [77].

Solid-phase extraction is a column-filling extraction technique that makes use of specific fillers such as C_8 and C_{18} as sorbents. Girault et al. [78] combined microfluidic solid-phase extraction with stepwise gradient elution followed by online electrospray ionization-mass spectroscopy detection for the analysis of low concentrations of peptides. The method used C_8- and C_{18}-coated MBs as solid-phase extractants and allowed for rapid sorbent replacement with a simple rinse when the external magnetic field was turned off or removed, the detection limit of the device for insulin was 10 nmol/L (Figure 4b). The team [79] also used C_8-functional mesoporous magnetic microspheres (C_8-Fe_3O_4@mSiO_2) as a sorbent, which had noticeably better peptide adsorption than commercial C_8-coated magnetic spheres. In contrast, $C_8-Fe_3O_4$@mSiO_2 microspheres possess a larger specific surface area and higher loading capacity. This MNPs-based microfluidic solid-phase extraction technique still essentially used conventional reversed-phase fillers as sorbents for the separation of analytes.

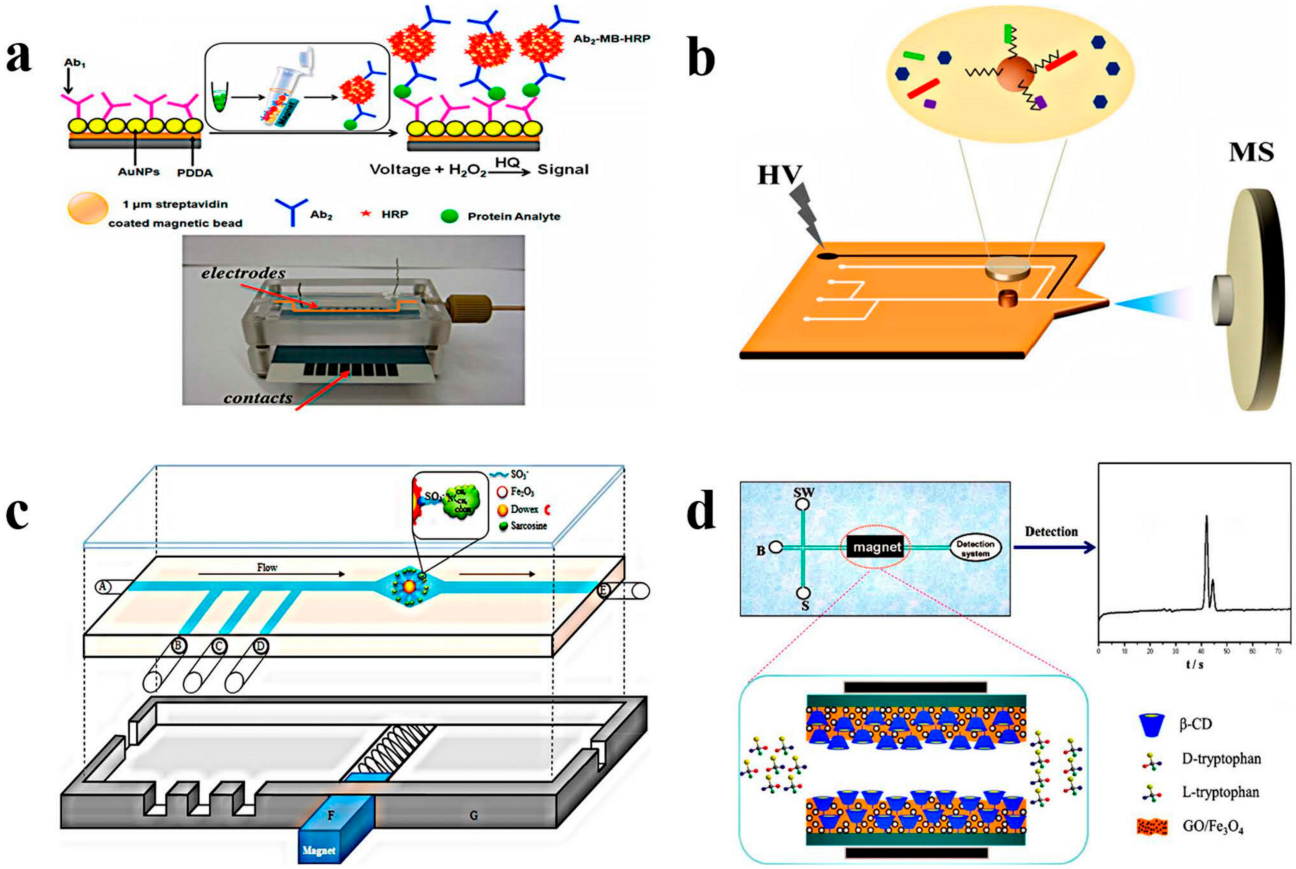

Figure 4. Magnetic separation strategies in MNPs-assisted microfluidic bioassays. (**a**) Schematic illustration of MSPE, copied with permission [68], copyright © 2012 American Chemical Society. (**b**) Schematic illustration of SPE on a chip, copied with permission [78], copyright © 2013 American Chemical Society. (**c**) Schematic illustration of ion exchange separation on a chip, copied with permission [80], copyright © 2013 WILEY-VCH Verlag GmbH & Co. KGaA, Weinheim. (**d**) Schematic illustration of chromatographic separation on a chip, copied with permission [81], copyright © 2012 Elsevier B.V.

Microfluidic systems combined with ion exchange separation and chromatographic separation techniques have also been used to separate analytes. Adam et al. [80] reported a microfluidic system based on modified paramagnetic particles for sarcosine separation and subsequent analysis on ion exchange liquid chromatography, which minimized the sample pretreatment requirements. The surface of Dowex 50WX4-400 microbeads, which contain SO_3^- functional groups, was modified with Fe_2O_3 nanoparticles to produce the paramagnetic particles. Partial modification of the surface of the microbeads eliminated the adsorption of unwanted biomolecules (Figure 4c). Qiu et al. established an open-tube capillary electrochromatography chip for enantiomer selective separation and detection. Using a magnetic nanocomposite (GO/Fe_3O_4 NCS) as the stationary phase, the chip was utilized to perform chiral splitting of the tryptophan enantiomers. This was followed by in-column electrochemical detection with detection limits of 7.6 and 9.5 μmol/L for D-tryptophan and L-tryptophan, respectively [81] (Figure 4d). A highly accurate size-based microparticle separation technique called "rotating magnetic chromatography" was developed for the separation of microparticles by Li et al. [82]. This novel technique exploited the interaction between MNPs and particles, where the MNPs moved in a specific trajectory due to an external magnetic field, while the particles flowed through a microfluidic separation channel and were separated according to size. The method was successfully applied to the analysis of cancer cells SK-HEP-1 and HEP-3B. Due to its unparalleled ability to isolate submicron

cells, rotating magnetic chromatography can be considered a breakthrough technology that can unlock new perspectives in medical oncology.

3.1.2. Microfluidic Magnetic Enrichment

Enrichment of the analytes is necessary after the analytes are separated from the sample solution during sample preparation. Hence, magnetic separation and enrichment are frequently combined. Magnetic enrichment improves the sensitivity of biomedical diagnostics by increasing the concentration of biomedical samples. MNPs were successfully used in microfluidic systems to magnetically separate and concentrate trace analytes such as DNA [83], estrogens [84], circulating tumor cells [85], genomic DNA [86], etc., where analyte loss was decreased and enrichment effectiveness was increased. Additionally, magnetic separation and pre-concentration processes could be conducted in the centrifugal tube off-chip, and purified analytes are then submitted to a microfluidic sensing system to detect (e.g., electrochemical assays [87], fluorescence assays [88], surface-enhanced Raman spectroscopy assays [89], and surface plasmon resonance assays [90]). The sensors see only the analyte and/or microbeads and never contact the full sample to limit nonspecific binding. A novel "all-in-one" approach that combines magnetic separation, enrichment, and detection of samples on a chip to meet the needs of point-of-care detection was presented to speed up the separation and analysis. The "all-in-one" approach was successfully used to detect thrombin [91], glucose [92], peptides [93], carcinoembryonic antigen, and Alpha-fetoprotein [94], the approach possesses the strengths of rapid and highly sensitive detection, no pre-treatment or low pre-treatment requirements. To identify microRNAs rapidly and with high sensitivity, Xing et al. [95] developed an electrochemiluminescence microarray system based on base stacking hybridization and magnetic particle enrichment techniques. The system combined microfluidics with electrochemiluminescence detection, allowing the construction of easily portable devices. The method did not require an enzymatic amplification effect and had a detection limit of 0.78 ng/mL for microRNA. (Figure 5a). Following an enzymatic amplification effect and gold nanoparticle amplification method, Oliveira et al. [96] developed a microfluidic electrochemical sensor based on immunomagnetic nanoparticles that detected prostate antigen down to 0.062 fg/mL. Nucleic acid amplification steps such as polymerase chain reaction or reverse transcription loop-mediated isothermal amplification could also be integrated into an "all-in-one" strategy for the successful detection of a trace amount of circulating cell-free DNA [22], H1N1 virus RNA [97]. Notably, a powerless, instrument-free "all-in-one" platform was better suited for point-of-care detection. When the target oligonucleotide was present, a magnetic particle-target-polystyrene particle sandwich structure was formed. The MBs captured the target to be measured and then preconcentrated in the capture zone, and the free polystyrene particles accumulated downstream of the microchip, forming visual strips of quantifiable length, the number of which was inversely proportional to the number of targets. Such an instrument-free and power-free platform enabled a limit of detection of oligonucleotides down to 13 fmol/L [98]. Similarly, Cui et al. [99] reported an economical and simple biosensing method. Competition analysis between MNPs, C-reactive protein antigens, and particles was used to quantify C-reactive protein concentrations. When C-reactive protein antigen was present, fewer MNPs bond to antibody-coupled particles, allowing the free particles to flow and be captured in a microfluidic particle accumulation chip after magnetic separation, forming a visual bar of quantifiable length, which is proportional to the concentration of C-reactive protein. A two-step competition method was applied to further improve the sensitivity and specificity of the assay with a detection limit of 32 pg/mL.

Electrochemical sensing signals are activated and amplified by the preconcentration of MNPs on microchips. Typically, biomolecules are immobilized on electrodes (such as gold or glassy carbon electrodes) to create electrochemical immunosensors, and MNPs are immobilized on the electrode surface to build magnetic electrodes. Signal tags for electrochemical immunosensors are commonly made of electrochemically active mate-

rials, which are bound and magnetically enriched on the sensor surface. Yi et al. [100] developed a regenerable electrochemical immunosensor in which an MBs-amino-terminal brain natriuretic peptide pro-Fab antibody-platinum Prussian blue nanomaterial sandwich compounds were magnetically enriched and fixed on the electrode surface, opening the sensor circuit. The electrochemical sensor had a detection limit of 0.003 ng/mL for amino-terminal brain natriuretic peptide pro-Fab antibody. Washing and regenerating the immunosensor with the magnet removed enabled continuous detection (Figure 5b). Similarly, silver-polypyrrole [101] and ferrocene [102] are also electrochemical active materials. Enzymes are also used as labels in electrochemical immunosensors for signal amplification. Chiou et al. [103] attached alginate microspheres containing magnetic powder and enzymes on the surface of the electrochemical sensor to detect various blood testing targets by switching different types of enzymes, which can solve the problem of enzyme preservation in a microfluidic device. More researchers used capture antibodies-labeled MBs to enrich analytes and formed sandwich complexes with detection antibodies-labeled horseradish peroxidase, which were immobilized on the electrode surface by an external magnetic field to achieve signal amplification [30]. Based on this, prostate cancer biomarkers [104] and severe acute respiratory syndrome coronavirus 2 [105] were rapidly and sensitively detected. Furthermore, Baldrich et al. [106] reported an electrochemical point-of-care system with sample preparation and detection of magnetic immunoassay on a disposable paper electrode microfluidic device with a detection limit of 2.47 ng/mL for plasmodium falciparum lactate dehydrogenase. The method requires little user intervention for quantitative diagnosis of malaria, which is not possible with other diagnostic methods.

Similarly, optical signals can be amplified by preconcentrating MNPs on microchips. Fluorescence detection signals are typically amplified via magnetic enrichment. Chuang et al. [107] created an open-well microfluidic fluorescent immunoassay platform where immune complexes made of MBs, tumor necrosis factor, and fluorescent dye-labeled detection antibodies gathered under magnetic force to form dense clusters with a detection limit of 2.9 pg/mL, and an open configuration facilitated user operation in different bioassays. The influenza virus [108] and free folate receptor [109], two trace analytes, were effectively found using a similar methodology. Using horseradish peroxidase rather than fluorescent dye, Li et al. [110] were able to achieve the dual fluorescence amplification effect of magnetic aggregation and horseradish peroxidase catalysis with detection limits of 0.29 pg/mL, 0.047 pg/mL, and 0.021 pg/mL for carcinoembryonic antigen, prostate-specific antigen, and interleukin-6, respectively (Figure 5c). The group further combined the microfluidic magnetic spatial confinement strategy to achieve triple amplification of the fluorescence signal with a detection limit of 2 cells/mL for human breast cancer cells MCF-7 [111]. Additionally, Baldrich et al. [112] developed a disposable microfluidic paper-based device and a handheld fluorescence reader, which enabled point-of-care detection.

The surface-enhanced Raman spectroscopy signal can also be amplified by magnetic preconcentration [113]. Noble metal nanoparticles [114] and Raman-active nanoparticles [115] are commonly used as Raman tags. Additionally, by substituting Raman reporter molecules (such as 5,5-dithio-bis-(2-nitrobenzoic acid), para-mercaptobenzoic acid) modified noble metal nanomaterials for the naked noble metal nanoparticles, the simultaneous detection of multiple analytes was made possible [116]. Based on this, catalytic hairpin assembly technology combined with the magnetic aggregation signal amplification technique to achieve the dual signal amplification effect of surface-enhanced Raman spectroscopy [117,118]. Furthermore, a surface-enhanced Raman spectroscopy-based microdroplet sensor created by Choo et al. greatly increased the sensitivity and reproducibility of the detection of severe acute respiratory syndrome coronavirus 2, with a limit of detection and coefficient of variation rising from 36 PFU/mL to 0.22 PFU/mL, and 21.2% to 1.79%, respectively [119]. Traditional surface plasmon resonance technology finds it challenging to directly detect low-concentration analytes, but magnetic enrichment can enhance the surface plasmon resonance signal [120].

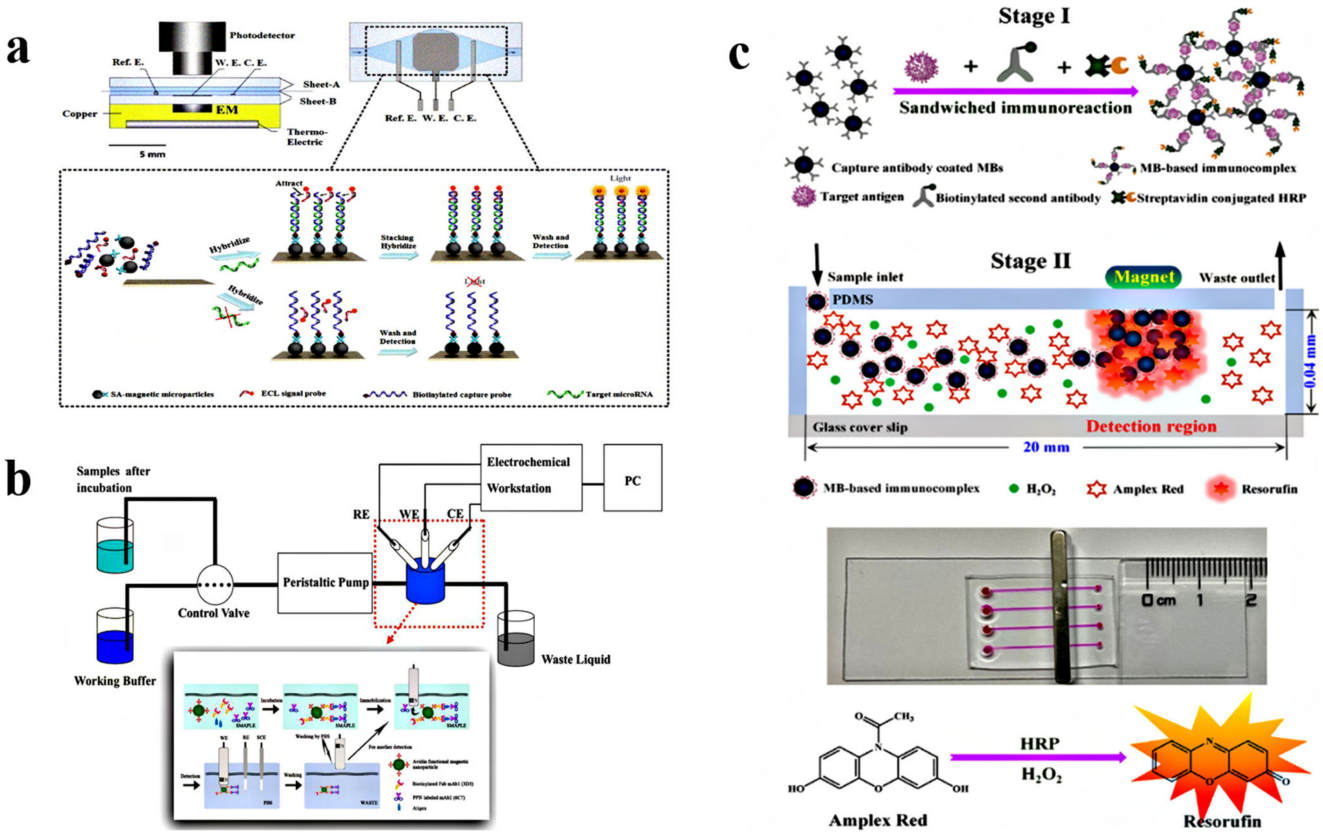

Figure 5. "All in one" strategy for magnetic separation, enrichment, and detection in MNPs-assisted microfluidic. (**a**) Schematic illustration of magnetic enrichment and detection on a microfluidic chip, reproduced with permission from ref [95], copyright © 2014 Elsevier B.V. (**b**) Schematic illustration of magnetic preconcentration on microchips to turn on electrochemical sensing signals, reproduced with permission from ref [100], copyright © 2011 Elsevier B.V. (**c**) Schematic illustration of magnetic preconcentration on microchips to amplify fluorescence detection signals, reproduced with permission from ref [110], copyright © 2021 American Chemical Society.

3.1.3. Microfluidic Magnetic Transport

Driven by magnetic force, MNPs allows analytes to transport and mix in an automated manner, saving human labor and enhancing sample preparation efficiency, and promising the integration and full automation of sample preparation and detection [121]. Digital microfluidics, also known as droplet microfluidics, are typical examples of microfluidic magnetic transport. On the one hand, it is the transport of droplets. The first digital microfluidic electrochemical immunosensor, described by Wheeler et al. [122], utilized a sequential flow of sample and immunoreactive reagent droplets across MNPs to capture and detect thyroid hormone with a detection limit of 2.4 μIU/mL. The simplicity and small size of the detector is a potential application for future portable analysis. Rühe et al. [123] reported a droplet microfluidic device that was founded on a sandwich immunoassay. Based on droplet motion, a switchable magnetic trap was added to repeatedly catch and release MNPs, allowing for the sequential analysis of multiple samples and a two order of magnitude increase in extraction efficiency of MNPs from aqueous nanoliter-sized drops over traditional enzyme-linked immunoassay. The platform offers strong advantages in areas where sample and/or reagent volumes are limited and high throughput analysis is required. (Figure 6a). Droplets can serve as reaction chambers as well [124]. Zhou [125] developed a droplet digital polymerase chain reaction technology. The technique performed droplet digital polymerase chain reaction on droplets containing magnetic beads-prostate specific antigen-DNA immune complexes and was capable of detecting prostate-specific

antigen as low as 0.48 ng/mL. On the other hand, it is the transport of MBs. Kang et al. [126] described a droplet immunoassay microchip that consists of chambers storing water-based reagents for continuous analytical procedures, with a detection limit of 20 pg/mL for oligomeric amyloid β, the MBs were transported along the chamber to reduce nonspecific adsorption. The platform could be used for point-of-care testing as well as high-throughput clinical diagnostics (Figure 6b). Similarly, Liu et al. developed a chemiluminescent immunoassay system based on an active droplet array microfluidic chip. The automated chemiluminescence detection of procalcitonin may be accomplished in less than 12 min by driving the MBs to move and react along a sequence of droplets that were pre-loaded with reagents with a detection limit of 0.044 ng/mL [127]. The entire analysis can be carried out flexibly in droplets containing MBs by fine-tuning the magnetic density to alter the extraction of the beads (<320 mT) and the delivery of the droplets (>320 mT) [128]. In addition, the sensitivity of the assay is increased by combining digital microfluidics with the nucleic acid amplification techniques isothermal cycling to cyclic amplification [129], reverse transcription-polymerase chain reaction [130], and digital polymerase chain reaction [131]. Analytical efficiency is improved by coupling a simple and flexible droplet microfluidic sample preparation technique with a nucleic acid amplification procedure. Interestingly, a microfluidic chip successfully achieves quick and automated detection of C-reactive protein by magnetically deflecting MBs laterally across alternating laminar flow streams of reagents and washing with a detection limit of 0.87 μg/mL. The platform eliminated the multiple manual steps and long diffusion-based reaction times required for off-chip magnetic bead analysis and enzyme linked immunosorbent assay with analysis speeds of less than 60 s [132].

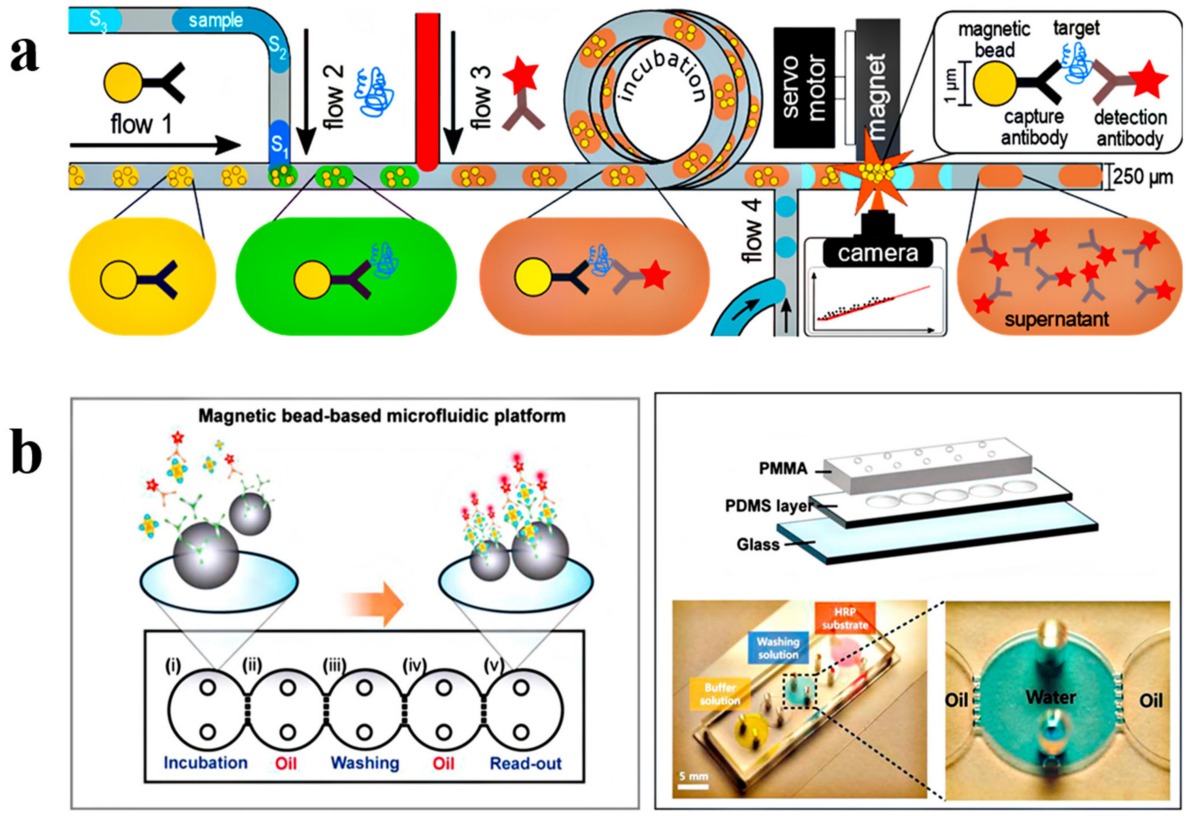

Figure 6. Microfluidic magnetic transport. (**a**) Schematic illustration of droplet transport-based microfluidic system, reused with permission from ref [123], copyright © 2020 American Chemical Society. (**b**) Schematic illustration of droplet microfluidic platform based on MBs transport, reused with permission from ref [126], copyright © 2014 Elsevier B.V.

More research on MNPs transport is based on a sophisticated microfluidic chip design, where a series of chambers are pre-loaded with the substances required for a sequential immune reaction, and MNPs are moved through the series of chambers under magnetic force. This method automates the reaction process without the use of pumps or large machinery and has great potential for application in rapid clinical diagnostics at the point of care. See Table 2 for more research on the transport of MNPs. MNPs can also serve as magnetic stirrers. Magnetic mixing, as opposed to passive mixing, improves the possibility of contact between MNPs and analytes, leading to a significantly higher speed and sensitivity [133]. The migration of magnetic beads has led to a breakthrough in the miniaturization and automation of microfluidic immunoassays. Based on the migration of magnetic beads, all analytical steps can be performed on a closed microchip, which facilitates the requirements of rapid, sensitive, and portable analysis for different assay scenarios.

Table 2. Studies on the transport of MNPs.

Manipulation	Functional MNPs	Sample	Analyte	Detection Method	LOD	Time/min	Point-Of-Care	Ref
Automated	MBs	nasopharyngeal swab	H1N1 RNA	RT-PCR	26 copies	60	No	[134]
	iron oxide functionalized NPs	nasopharyngeal swabs and saliva	SARS-CoV-2	RT-PCR	-	<15	No	[135]
	antibody conjugated MBs	erythrocyte solution	H1N1	FL	5.1×10^{-4} HAU	33	No	[136]
	antibody-coated MBs	plasma	ZIKV NS1	CO	62.5 ng/mL	10	Yes	[137]
	paramagnetic surface-oxidized nickel nanoparticles (Ni/NiO NPs)	-	SP	CO	10^5 CFU/mL	15	No	[18]
	DNA target complex on MBs	-	DNA	OM	2 pmol/L	45	No	[138]
	antibody-bound dynabeads	serum	CRP	CL	1.5 ng/mL	25	Yes	[139]
	capture antibody labeled MBs	cell lysate	CEA, EGFR	FL	0.82×10^{-5} ng/mL	120	No	[140]
	antibody conjugated MBs	blood	IL-6, TNF-α	FL	1×10^{-3} ng/mL	20	No	[141]
	p53 antigen conjugated MBs	saliva	anti-p53 autoantibody	CO	4 ng/mL	60	No	[142]
non-automated	cellulose functionalized MBs	plasmid	HPV 18	RT-PCR	50 copies	<15	No	[143]
	antibody functionalized MBs	-	β-hCG	EC	10 ng/mL	31	Yes	[144]
	capture antibody-conjugated MBs	serum	HIV-1p24	VS	0.5 ng/mL	60	Yes	[145]
	capture antibody-conjugated MBs	serum	CRP, PSA	VS	10 ng/mL	120	No	[146]
	antibody-coated MBs;	serum	TNF-α	imaging	1×10^{-6} ng/mL	20	No	[147]
	primary antibody-conjugated MNPs	serum	PSA	imaging	3.2 ng/mL	45	No	[148]

LOD, the limit of detection; RT-PCR, reverse transcription-polymerase chain reaction; FL, fluorogenic; CO, colorimetric; OM, opto-magnetic; CL, chemiluminescence; EC, electrochemical; VS, visual; ZIKV NS1, zika virus nonstructural protein 1; SP, *Streptococcus pneumoniae*; IL-6, interleukin-6; HPV, human papillomavirus; β-hCG, β-type human chorionic gonadotropin; HIV, human immunodeficiency virus; HSV, herpes simplex virus; TNF-α, tumor necrosis factor-α; HAU, hemagglutination units; CFU, colony-forming units; -, not mentioned.

3.2. MNPs for Biosensing

Biosensors are analytical devices or systems that detect specific targets by converting and amplifying biomolecular recognition events into signals that can be semi-quantified or quantified. The recognition sensing element can be classified according to their interactions with analytes, including antibody-antigen, nucleic acid, aptamers or peptides and corresponding targets, enzyme-substrate, ligand-receptor, and host-guest interactions. Common forms of signal transduction utilized in biosensing include electrochemical, optical, magnetic, and surface plasmon resonance transducers, etc. [149]. For biosensing, the magnetic response is the unique advantage of MNPs, such as magneto-resistive and magnetic relaxation. These specific magnetic responses combined with microfluidic chip devices have been applied in bioanalysis. In addition, using MNPs as a supporter, optical sensing labels can be immobilized and easily handled with an external magnet.

3.2.1. Microfluidic Magnetic Biosensors

The microfluidic magnetic sensor is an analytical device on a microfluidic chip utilizing MNPs as bio-conjugated carriers and/or magnetic tags. There are two analytical principles for microfluidic magnetic sensors, one based on the presence or absence of MNPs on the sensor surface. As shown in Figure 7a, functional group A is modified on the surface of the magnetic sensor, and MNPs labelled with functional group B are mixed with the biological sample to specifically bind the targets, which are transported to the sensing region and form a magnetic immune complex with functional group A. The stray field of a magnetically labeled bio-analyte is detected by a magnetic sensor. The other is based on the analysis of the aggregation and dispersion states of MNPs. As seen in Figure 7b, MNPs labeled with functional groups exhibit two different states of aggregation and dispersion in the presence and absence of targets, causing signal changes in themselves or surrounding molecules, which are detected by the magnetic sensors. Magnetic sensors offer several key advantages, such as the ability to rapidly detect target molecules; no noise is detected during magnetic signal capture; as well as key benefits such as small size, low cost, high sensitivity, and biocompatibility.

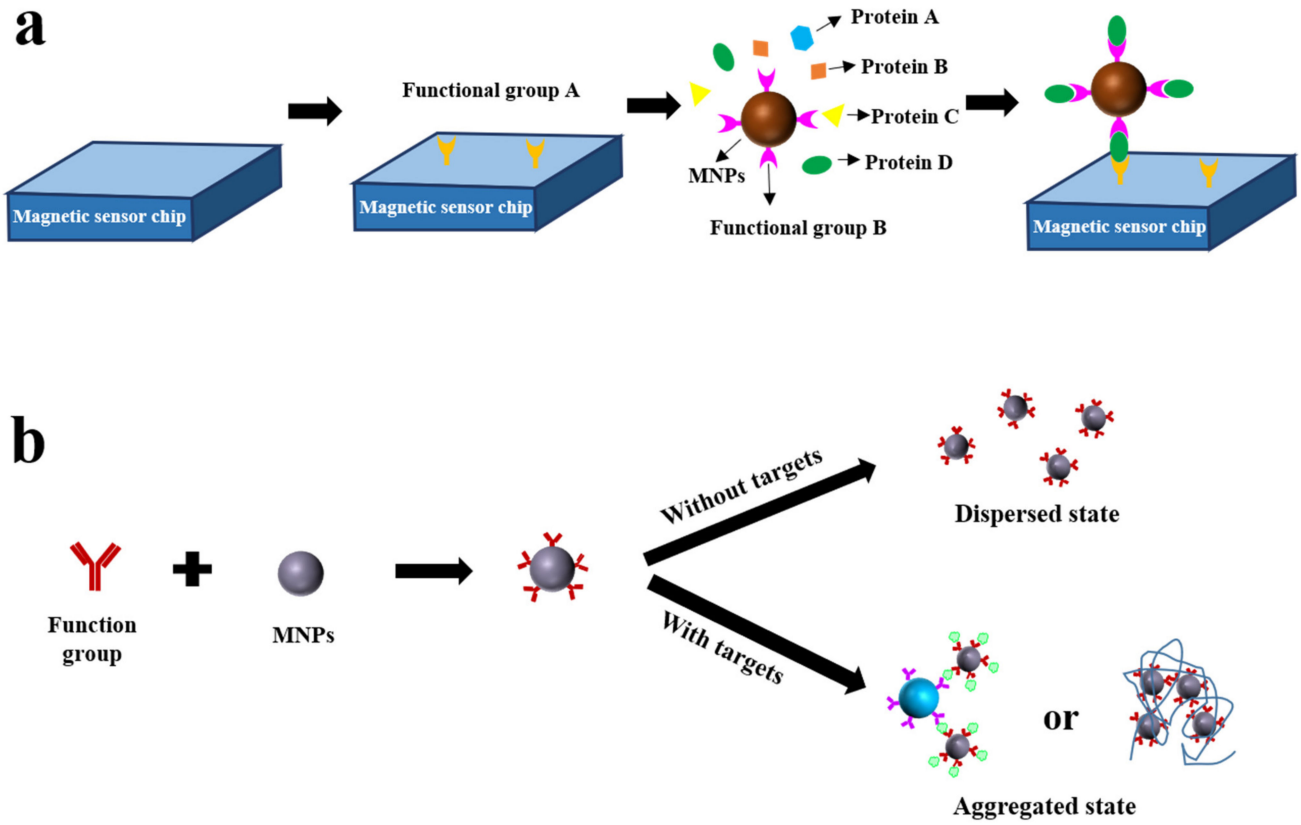

Figure 7. Principle of microfluidic magnetic sensors. (**a**) Analysis based on the presence or absence of MNPs on the sensor surface. (**b**) Analysis based on the dispersion and aggregation state of MNPs.

The magneto-resistive effect is the change in resistance when a magnetic field is applied. Magneto resistive sensor is analyzed based on the presence or absence of MNPs on the sensor surface. A magnetic field is applied above the magneto resistive sensor and the magnetic nanoparticles bound to the surface of the sensor are magnetized, creating a stray magnetic field that causes a change in the resistance of the sensor [150]. Giant magneto-resistive sensors are the most widely used magnetic sensors. MNPs can be bound to the sensor surface by two methods: direct immunoassay and double antibody sandwich method. Cui et al. reported a microfluidic platform incorporating a giant magneto resistive sensor, which was detected by direct immunoassay by trapping streptavidin-

modified magnetic nanoclusters onto biotin-labeled hybridization products at the sensor interface, resulting in a switch in the resistance of the sensor with a detection limit of 200 IU/mL [151]. For efficient amplification of the analyte, loop isothermal amplification was used instead of polymerase chain reaction with a detection limit of 10 copies/mL for hepatitis B virus DNA [152]. MNPs can also be bound to the giant magneto resistive sensor surface using a dual antibody sandwich method. Wang et al. established a simple and sensitive method for the detection of the influenza A virus. A monoclonal antibody against the viral nucleoprotein was bound to MNPs, and the presence of the virus allowed the MNPs to bind to the captured antibody on the surface of the giant magneto resistive sensor, resulting in a change in the resistance of the sensor [153]. The group further integrated a portable point-of-care device, a platform that allows testing outdoors and can be applied in non-clinical settings [154]. To further enhance the field diagnostic capabilities of the platform, the group further developed a wash-free magnetic bioassay [155]. In addition, an "all-in-one" strategy enabled the portable, low-cost, and sensitive detection of cytosolic fibronectin, matrix metallopeptidase 9 [156], and 12 tumor markers [157]. Compared with giant magneto resistive sensors, magnetic tunnel junction sensor has a higher signal-to-noise ratio [158]. Petti reported a portable electronic and microfluidic platform based on compact magnetic tunnel junctions sensing device that successfully achieved ultra-sensitive detection of *Listeria monocytogenes* DNA below the nanomolar range [159] (Figure 8a).

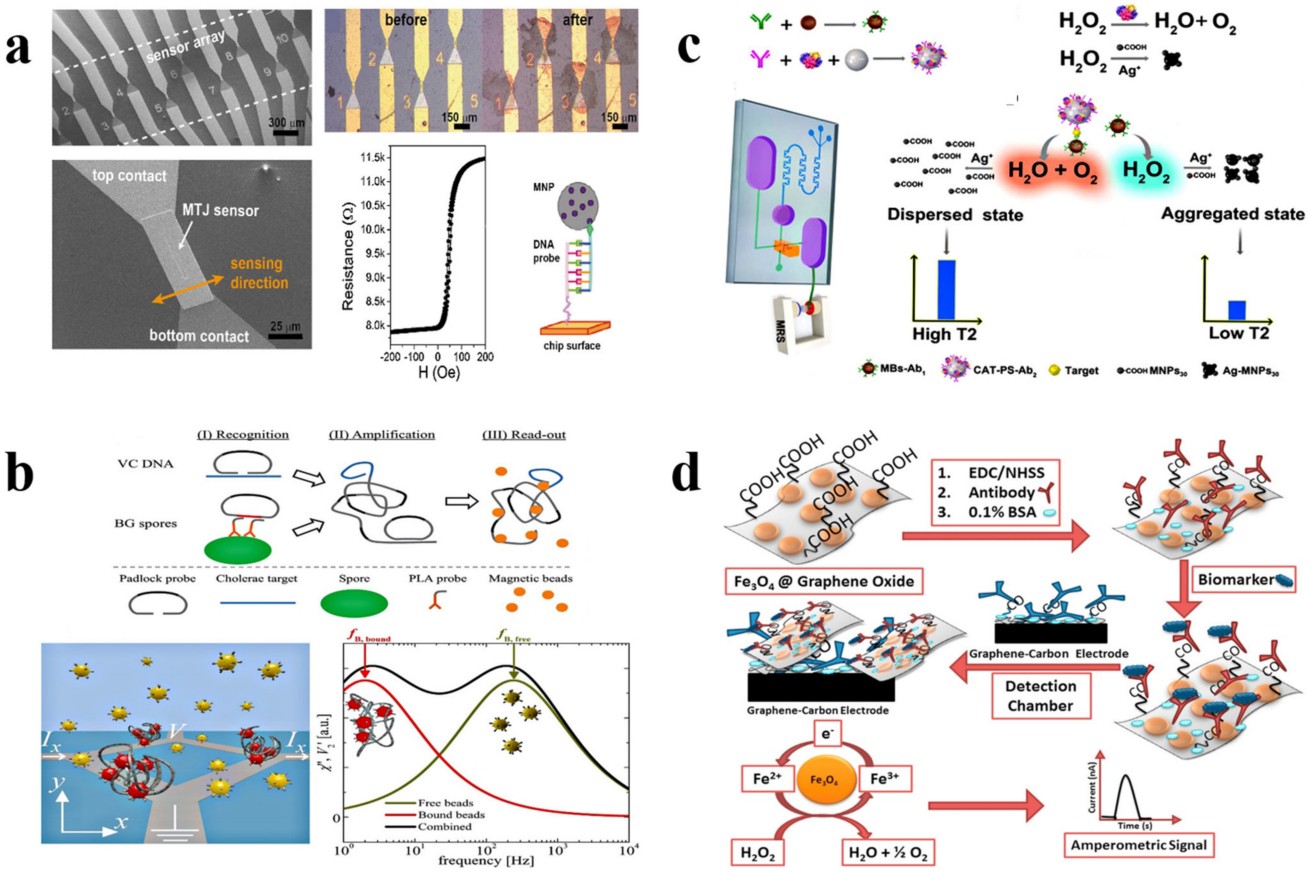

Figure 8. Microfluidic magnetic biosensors. (**a**) Schematic illustration of MTJ biosensor integrated microfluidic chip, adapted with permission from [159], copyright © 2016 Elsevier B.V. (**b**) Schematic illustration of the magnetic relaxation switching sensor, reprinted with permission from [160], copyright © 2021 Frontiers Media. (**c**) Schematic illustration of the Brownian relaxation sensor, reprinted with permission from [161], copyright © 2014 WILEY−VCH Verlag GmbH & Co. KGaA, Weinheim. (**d**) Schematic illustration of protein capture and detection mediated by Fe_3O_4@GO sheets, reprinted with permission from [162], copyright © 2016 Elsevier B.V.

The giant magnetic impedance effect is the variation of the alternating current impedance when the applied direct current magnetic field changes. The giant magnetic impedance sensor is similarly analyzed based on the presence or absence of MNPs on the sensor surface. Giant magnetic impedance sensors are more sensitive and respond more quickly than other traditional magnetic sensors. Feng et al. [163] proposed an integrated microfluidic device based on a giant magnetic impedance sensor, where prostate-specific antigen was coupled to antibody-labeled MNPs and captured onto the Au membrane surface, and the captured MNPs generated a stray magnetic field under an applied direct current magnetic field, resulting in a significant change in the alternating current impedance of the giant magnetic impedance sensor with a detection limit of 0.1 ng/mL. Furthermore, Kim et al. proposed a novel portable impedance biosensor platform for the sensitive detection of human tumor necrosis factor α, which can be used for digital diagnosis for real sample-in result-out systems [164]. To reliably and sensitively detect glial fibrillary acidic protein to distinguish brain hemorrhage from acute ischemic stroke, a compact microfluidic magnetic impedance biosensor was developed for the detection of glial fibrillary acidic protein in biological samples with a detection limit of 1.0 ng/mL [165].

Part of the magnetic sensor is based on the analysis of the aggregation or dispersion of MNPs. The magnetic relaxation switching sensor is based on the effect of MNPs on the relaxation rate of water protons [166]. When MNPs form target-induced aggregates, the transverse relaxation time (T_2) of adjacent water protons is changed. Yi et al. developed a microfluidic nuclear magnetic resonance detection device for the rapid detection of tumor markers [167]. Yin et al. reported a microfluidic chip-based magnetic relaxation switch immunosensor that simplified manipulation and amplified the detection signal of samples by enzyme-mediated nanoparticles. CAT-PS-AB2 was prepared by simultaneously labeling peroxidase (CAT) and detection antibody (AB2) on polystyrene (PS) microspheres. The targets were specifically bound to antibodies modified on MBs and polystyrene, respectively, to form sandwich structures. The degree of aggregation of Ag-$MNPs_{30}$ was regulated by the decomposition of H_2O_2 by catalase, which caused a change in the lateral relaxation time (T_2). The sensor was successfully applied to the detection of alpha-fetoprotein in real samples with a detection limit of 0.56 ng/mL (Figure 8b) [160]. The theory behind the Brownian relaxation sensor is that MNPs form target-induced aggregates with a larger hydrodynamic radius and exhibit a slower Brownian relaxation response than individual MNPs do. Hansen et al. performed the first Brownian relaxation measurements on magnetic nanorods on a chip using magneto-resistive sensors for the quantification of *Bacillus globigii spores* and *Vibrio cholerae* on DNA coils formed by rolling circle amplification. The free MBs have a higher Brownian relaxation frequency $f_{B,\,free}$, while the MBs bound to the rolling circle amplification coil have a larger hydrodynamic size, significantly lowering the Brownian relaxation frequency f_B. The proportion of MBs bound to the rolling circle amplification coil depends on the concentration of the rolling circle amplification coil (Figure 8c) [161]. To achieve truly low-cost and high-performance analysis, the group developed a new Blu-ray optical pick-up unit to measure the Brownian rotational dynamics of MBs [168]. The team went on to successfully detect C-reactive protein using a lab-on-a-disc platform in a sensitive and fully automated manner [169].

3.2.2. MNPs-Assisted Optical Microfluidic Biosensors

MNPs-assisted optical microfluidic sensors consist of a biological recognition component that interacts or reacts with the biological analyte studied and an optical sensor that converts that recognition component into a measurable electrical output signal in a microfluidic system using magnetic nanoparticles as a signal tag.

Most investigations rely on either imaging MBs during an aggregation test or imaging MBs that have been fluorescently probe-labeled since light microscopy cannot capture individual MBs with sufficient clarity. To quickly detect *Clostridium difficile* using a mobile phone camera, Landers et al. [170] paired an MBs aggregation test with a microfluidic device. The platform relied on the inhibition of MBs aggregation by long DNA strands,

which normally induce bead aggregation under hybridization conditions in rotating magnetic fields. This technique was coupled to loop-mediated isothermal amplification that effectively eliminated the requirement for thermal cycling. The bead aggregation test served as the foundation for the development of a low-cost, high-throughput "windmill test" platform with a detection limit of 5 pg/chamber for human genomic DNA [171]. Lee et al. [172] suggested an asymmetric immune aggregation test with a detection limit of 40 pg/mL for the quick, label-free detection of influenza A nucleoprotein. Additionally, MNPs were employed as signal markers, fixed at particular sites in the microchannel by immunoassay, counted, and photographed using a fluorescence microscope [173] or complementary metal oxide semiconductor camera [174]. Fluorescence imaging with MBs trapping was used in part of the study for quantitative analysis. Guo [175] used MagPlex® color-coded beads to simultaneously detect several cancer biomarkers, which may be conducted with the aid of 500 sets of MagPlex® color-coded beads in the same microchamber. The β-galactosidase/N protein/antibody-labeled MBs immunocomplex was constrained to fly-liter-sized wells, each carrying only one bead. A fluorescent substrate reaction was then added to produce a locally high concentration of fluorescent product with a detection limit of 33.28 pg/mL for protein, which was 300 times lower than that of a standard enzyme-linked immunoassay [176].

Additionally, MNPs can be utilized as Raman labels and enzyme tags for optical detection. MNPs exhibit inherent peroxide-like mimetic enzyme activity but are poorly dispersed. Using the dispersion of carbon (C) and the high catalytic activity of palladium nanoparticles (Pd), Yu et al. [177] developed Pd/Fe_3O_4@C magnetic nanocomplexes with high catalytic activity against 3,3′,5,5′-tetramethylbenzidine and o-phenylenediamine chromogenic substrates. They also built a paper-based microfluidic multiplexed colorimetric immunoassay apparatus with a detection limit of 1.7 pg/mL for the quick and inexpensive simultaneous detection of carcinoembryonic antigen and Alpha-fetoprotein. To increase the hydrophilicity and dispersibility of MNPs, Rusling et al. [162] placed Fe_3O_4 nanoparticles on graphene oxide nanosheets. As a result, they were able to detect prostate-specific antigen and prostate-specific membrane antigen by an ultra-sensitive electrochemical method with low-cost detection limits of 15 fg/mL and 4.8 fg/mL, respectively (Figure 8d). $Co_{0.25}Zn_{0.75}Fe_2O_4$ (CoZn-FeONPs) magnetic nanocomplexes were created by Faria [178] in order to further enhance the catalytic activity of MNPs. They were then put into a disposable enzyme-free microfluidic immune array device for the electrochemical detection of cytokeratin fragment antigen 21-1 with a detection limit as low as 0.19 fg/mL. Huang et al. [179] created a type of magnetic multicolor surface-enhanced Raman scattering nanotag (IO-Au Raman nanotags), multiple surface protein markers for magnetic capture, and simultaneous detection of a single tumor cell. The dual enrichment and detection capabilities of magnetic-plasmonic nanoparticles were exhibited.

4. Conclusions and Prospects

To summarize, the MNPs-assisted microfluidic bioanalysis is showing excellent analytical performance in selectivity, sensitivity, and speed. Moreover, the introduction of functionalized MNPs enlarges the application scope of microfluidics, and the steerable properties of MNPs advance bioanalysis in an automated way. These MNPs can be used as sample pretreatment materials and/or biosensing tags. In sample pretreatment, the application of magnetic nanoparticles allows separation and concentration in one step, contributing to the development of wash-free, simple, rapid, and in-situ sample preparation techniques. In biosensing, magnetic nanoparticles have powerful potential for applications with multiple functions such as separation carriers and signal tags. Despite the rapid development of MNPs-assisted microfluidic bioanalysis in the last decade, there are still some issues that need to be addressed. Firstly, to suit the usage in microfluidic bioanalysis, the particle size, stability, and toxicity of the MNPs have to be taken into account in the material preparation. Secondly, more multifunctional MNPs capable of integration of several analytical processes are highly desired to further improve the analytical performance of

MNPs-assisted microfluidic bioanalysis. Thirdly, to push the practicality of MNPs-assisted microfluidic bioanalysis forward, more effort should be put into the further simplification of microfluidic devices and operations.

Author Contributions: Z.Z.: Methodology, Data curation, Investigation, Writing-original draft preparation.; J.H.: Visualization, Supervision; G.L.: Visualization, Resources, Funding acquisition, Supervision, Project administration, Writing—review & editing; L.X.: Visualization, Resources, Funding acquisition, Supervision, Project administration, Writing—review & editing. All authors have read and agreed to the published version of the manuscript.

Funding: This work was supported by the National Natural Science Foundation of China (Nos. 22076223, 21976213), the State Key Program of National Natural Science of China (No.22134007), the National Key Research and Development Program of China (No.2019YFC1606101), and the Research and Development Plan for Key Areas of Food Safety in Guangdong Province of China (No. 2019B020211001), respectively.

Institutional Review Board Statement: Not applicable.

Informed Consent Statement: Not applicable.

Data Availability Statement: Data sharing not applicable.

Conflicts of Interest: The authors declare no conflict of interest.

References

1. Fattahi, Z.; Hasanzadeh, M. Nanotechnology-assisted microfluidic systems for chemical sensing, biosensing, and bioanalysis. *Trends Analyt. Chem.* **2022**, *152*, 116637. [CrossRef]
2. Sharma, B.; Sharma, A. Microfluidics: Recent advances toward lab-on-chip applications in bioanalysis. *Adv. Eng. Mater.* **2021**, *24*, 2100738. [CrossRef]
3. Xia, L.; Yang, J.; Su, R.; Zhou, W.; Zhang, Y.; Zhong, Y.; Huang, S.; Chen, Y.; Li, G. Recent Progress in Fast Sample Preparation Techniques. *Anal. Chem.* **2019**, *92*, 34–48. [CrossRef] [PubMed]
4. Xia, L.; Li, G. Recent progress of microfluidics in surface-enhanced Raman spectroscopic analysis. *J. Sep. Sci.* **2021**, *44*, 1752–1768. [CrossRef]
5. Battat, S.; Weitz, D.A.; Whitesides, G.M. An outlook on microfluidics: The promise and the challenge. *Lab Chip* **2022**, *22*, 530–536. [CrossRef]
6. Chen, T.; Yin, S.; Wu, J. Nanomaterials meet microfluidics: Improved analytical methods and high-throughput synthetic approaches. *Trends Analyt. Chem.* **2021**, *142*, 116309. [CrossRef]
7. Xia, L.; Chen, X.; Xiao, X.; Li, G. Magnetic-covalent organic polymer solid-phase extraction coupled with high-performance liquid chromatography for the sensitive determination of fluorescent whitening agents in cosmetics. *J. Sep. Sci.* **2018**, *41*, 3733–3741. [CrossRef]
8. Zhou, L.; Hu, Y.; Li, G. Conjugated microporous polymers with built-in magnetic nanoparticles for excellent enrichment of trace hydroxylated polycyclic aromatic hydrocarbons in human urine. *Anal. Chem.* **2016**, *88*, 6930–6938. [CrossRef]
9. Zhang, H.; Lai, H.; Wu, X.; Li, G.; Hu, Y. $CoFe_2O_4$@HNTs/AuNPs substrate for rapid magnetic solid-phase extraction and efficient SERS detection of complex samples all-in-one. *Anal. Chem.* **2020**, *92*, 4607–4613. [CrossRef]
10. Khizar, S.; Ben Halima, H.; Ahmad, N.M.; Zine, N.; Errachid, A.; Elaissari, A. Magnetic nanoparticles in microfluidic and sensing: From transport to detection. *Electrophoresis* **2020**, *41*, 1206–1224. [CrossRef]
11. Shang, Y.; Xiang, X.; Ye, Q.; Wu, Q.; Zhang, J.; Lin, J.-M. Advances in nanomaterial-based microfluidic platforms for on-site detection of foodborne bacteria. *Trends Analyt. Chem.* **2022**, *147*, 116509. [CrossRef]
12. Gjergjizi, B.; Çoğun, F.; Yıldırım, E.; Eryılmaz, M.; Selbes, Y.; Sağlam, N.; Tamer, U. SERS-based ultrafast and sensitive detection of luteinizing hormone in human serum using a passive microchip. *Sens. Actuators B Chem.* **2018**, *269*, 314–321. [CrossRef]
13. Yap, L.W.; Chen, H.; Gao, Y.; Petkovic, K.; Liang, Y.; Si, K.J.; Wang, H.; Tang, Z.; Zhu, Y.; Cheng, W. Bifunctional plasmonic-magnetic particles for an enhanced microfluidic SERS immunoassay. *Nanoscale* **2017**, *9*, 7822–7829. [CrossRef]
14. Wang, R.; Zhao, R.; Li, Y.; Kong, W.; Guo, X.; Yang, Y.; Wu, F.; Liu, W.; Song, H.; Hao, R. Rapid detection of multiple respiratory viruses based on microfluidic isothermal amplification and a real-time colorimetric method. *Lab Chip* **2018**, *18*, 3507–3515. [CrossRef]
15. Ling, W.; Wang, M.; Xiong, C.; Xie, D.; Chen, Q.; Chu, X.; Qiu, X.; Li, Y.; Xiao, X. Synthesis, surface modification, and applications of magnetic iron oxide nanoparticles. *J. Mater. Res.* **2019**, *34*, 1828–1844. [CrossRef]
16. Hung, L.Y.; Chang, J.C.; Tsai, Y.C.; Huang, C.C.; Chang, C.P.; Yeh, C.S.; Lee, G.B. Magnetic nanoparticle-based immunoassay for rapid detection of influenza infections by using an integrated microfluidic system. *Nanomedicine* **2014**, *10*, 819–829. [CrossRef]
17. Gong, X.; Yan, H.; Yang, J.; Wu, Y.; Zhang, J.; Yao, Y.; Liu, P.; Wang, H.; Hu, Z.; Chang, J. High-performance fluorescence-encoded magnetic microbeads as microfluidic protein chip supports for AFP detection. *Anal. Chim. Acta.* **2016**, *939*, 84–92. [CrossRef]

18. Weng, C.C.; Chao, C.Y.; Wu, S.T.; Tsou, P.H.; Chen, W.T.; Li, B.R.; Li, Y.K. Integration of Ni/NiO nanoparticles and a microfluidic ELISA chip to generate a sensing platform for *Streptococcus pneumoniae* detection. *RSC Adv.* **2021**, *11*, 28551–28556. [CrossRef]
19. Bist, I.; Bhakta, S.; Jiang, D.; Keyes, T.E.; Martin, A.; Forster, R.J.; Rusling, J.F. Evaluating metabolite-related DNA oxidation and adduct damage from aryl amines using a microfluidic ECL array. *Anal. Chem.* **2017**, *89*, 12441–12449. [CrossRef]
20. Wang, W.; Huang, Y.; Jin, Y.; Liu, G.; Chen, Y.; Ma, H.; Zhao, R. A tetra-layer microfluidic system for peptide affinity screening through integrated sample injection. *Analyst* **2013**, *138*, 2890–2896. [CrossRef]
21. Wang, Z.; Fan, Y.; Chen, J.; Guo, Y.; Wu, W.; He, Y.; Xu, L.; Fu, F. A microfluidic chip-based fluorescent biosensor for the sensitive and specific detection of label-free single-base mismatch via magnetic beads-based "sandwich" hybridization strategy. *Electrophoresis* **2013**, *34*, 2177–2184. [CrossRef] [PubMed]
22. Perez-Toralla, K.; Pereiro, I.; Garrigou, S.; Di Federico, F.; Proudhon, C.; Bidard, F.-C.; Viovy, J.-L.; Taly, V.; Descroix, S. Microfluidic extraction and digital quantification of circulating cell-free DNA from serum. *Sens. Actuators B Chem.* **2019**, *286*, 533–539. [CrossRef]
23. Gimenez, T.D.; Bailão, A.M.; de Almeida Soares, C.M.; Fiaccadori, F.S.; Borges de Lima Dias e Souza, M.; Duarte, G.R.M. Dynamic solid-phase RNA extraction from a biological sample in a polyester-toner based microchip. *Anal. Methods* **2017**, *9*, 2116–2121. [CrossRef]
24. Li, B.; Pu, W.; Xu, H.; Ge, L.; Kwok, H.F.; Hu, L. Magneto-controlled flow-injection device for electrochemical immunoassay of alpha-fetoprotein on magnetic beads using redox-active ferrocene derivative polymer nanospheres. *Analyst* **2019**, *144*, 1433–1441. [CrossRef]
25. Liu, X.; Wang, F.; Meng, Y.; Zhao, L.; Shi, W.; Wang, X.; He, Z.; Chao, J.; Li, C. Electrochemical/visual microfluidic detection with a covalent organic framework supported platinum nanozyme-based device for early diagnosis of pheochromocytoma. *Biosens. Bioelectron.* **2022**, *207*, 114208. [CrossRef]
26. Tao, Y.; Pan, M.; Zhu, F.; Liu, Q.; Wang, P. Construction of a microfluidic platform with core-shell CdSSe@ZnS quantum dot-encoded superparamagnetic iron oxide microspheres for screening and locating matrix metalloproteinase-2 inhibitors from fruits of *Rosa roxburghii*. *Front. Nutr.* **2022**, *9*, 869528. [CrossRef]
27. Xie, L.; Li, T.; Hu, F.; Jiang, Q.; Wang, Q.; Gan, N. A novel microfluidic chip and antibody-aptamer based multianalysis method for simultaneous determination of several tumor markers with polymerization nicking reactions for homogenous signal amplification. *Microchem. J.* **2019**, *147*, 454–462. [CrossRef]
28. Grass, R.N.; Athanassiou, E.K.; Stark, W.J. Covalently functionalized cobalt nanoparticles as a platform for magnetic separations in organic synthesis. *Angew. Chem. Int. Ed. Engl.* **2007**, *46*, 4909–4912. [CrossRef]
29. Rossier, M.; Schreier, M.; Krebs, U.; Aeschlimann, B.; Fuhrer, R.; Zeltner, M.; Grass, R.N.; Günther, D.; Stark, W.J. Scaling up magnetic filtration and extraction to the ton per hour scale using carbon coated metal nanoparticles. *Sep. Purif. Technol.* **2012**, *96*, 68–74. [CrossRef]
30. Lei, J.; Shi, L.; Liu, W.; Li, B.; Jin, Y. Portable and sensitive detection of cancer cells via a handheld luminometer. *Analyst* **2022**, *147*, 3219–3224. [CrossRef]
31. Wang, C.; Ye, M.; Cheng, L.; Li, R.; Zhu, W.; Shi, Z.; Fan, C.; He, J.; Liu, J.; Liu, Z. Simultaneous isolation and detection of circulating tumor cells with a microfluidic silicon-nanowire-array integrated with magnetic upconversion nanoprobes. *Biomaterials* **2015**, *54*, 55–62. [CrossRef]
32. Horak, D.; Hlidkova, H.; Hiraoui, M.; Taverna, M.; Proks, V.; Mazl Chanova, E.; Smadja, C.; Kucerova, Z. Monodisperse carboxyl-functionalized poly(ethylene glycol)-coated magnetic poly(glycidyl methacrylate) microspheres: Application to the immunocapture of β-amyloid peptides. *Macromol. Biosci.* **2014**, *14*, 1590–1599. [CrossRef]
33. Singh, V. Ultrasensitive quantum dot-coupled-surface plasmon microfluidic aptasensor array for serum insulin detection. *Talanta* **2020**, *219*, 121314. [CrossRef]
34. Moura, S.L.; Fajardo, L.M.; Cunha, L.D.A.; Sotomayor, M.; Machado, F.B.C.; Ferrao, L.F.A.; Pividori, M.I. Theoretical and experimental study for the biomimetic recognition of levothyroxine hormone on magnetic molecularly imprinted polymer. *Biosens. Bioelectron.* **2018**, *107*, 203–210. [CrossRef]
35. Medina-Sanchez, M.; Miserere, S.; Morales-Narvaez, E.; Merkoci, A. On-chip magneto-immunoassay for Alzheimer's biomarker electrochemical detection by using quantum dots as labels. *Biosens. Bioelectron.* **2014**, *54*, 279–284. [CrossRef]
36. Zhao, X.; Huang, Y.; Li, X.; Yang, W.; Lv, Y.; Sun, W.; Huang, J.; Mi, S. Full integration of nucleic acid extraction and detection into a centrifugal microfluidic chip employing chitosan-modified microspheres. *Talanta* **2022**, *250*, 123711. [CrossRef]
37. Bettazzi, F.; Hamid-Asl, E.; Esposito, C.L.; Quintavalle, C.; Formisano, N.; Laschi, S.; Catuogno, S.; Iaboni, M.; Marrazza, G.; Mascini, M.; et al. Electrochemical detection of miRNA-222 by use of a magnetic bead-based bioassay. *Anal. Bioanal. Chem.* **2013**, *405*, 1025–1034. [CrossRef]
38. Du, K.; Cai, H.; Park, M.; Wall, T.A.; Stott, M.A.; Alfson, K.J.; Griffiths, A.; Carrion, R.; Patterson, J.L.; Hawkins, A.R.; et al. Multiplexed efficient on-chip sample preparation and sensitive amplification-free detection of Ebola virus. *Biosens. Bioelectron.* **2017**, *91*, 489–496. [CrossRef]
39. Wang, F.; Liu, Y.; Fu, C.; Li, N.; Du, M.; Zhang, L.; Ge, S.; Yu, J. Paper-based bipolar electrode electrochemiluminescence platform for detection of multiple miRNAs. *Anal. Chem.* **2021**, *93*, 1702–1708. [CrossRef]

40. Zhou, Q.; Lin, Y.; Zhang, K.; Li, M.; Tang, D. Reduced graphene oxide/$BiFeO_3$ nanohybrids-based signal-on photoelectrochemical sensing system for prostate-specific antigen detection coupling with magnetic microfluidic device. *Biosens. Bioelectron.* **2018**, *101*, 146–152. [CrossRef]
41. Noh, H.N.; Kim, J.S. Detection of K-Ras oncogene using magnetic beads-quantum dots in microfluidic chip. *J. Nanosci. Nanotechnol.* **2013**, *13*, 5240–5244. [CrossRef] [PubMed]
42. Mai, T.D.; Ferraro, D.; Aboud, N.; Renault, R.; Serra, M.; Tran, N.T.; Viovy, J.-L.; Smadja, C.; Descroix, S.; Taverna, M. Single-step immunoassays and microfluidic droplet operation: Towards a versatile approach for detection of amyloid-β peptide-based biomarkers of Alzheimer's disease. *Sens. Actuators B Chem.* **2018**, *255*, 2126–2135. [CrossRef]
43. Wang, C.H.; Chang, C.P.; Lee, G.B. Integrated microfluidic device using a single universal aptamer to detect multiple types of influenza viruses. *Biosens. Bioelectron.* **2016**, *86*, 247–254. [CrossRef] [PubMed]
44. Zheng, L.; Wang, H.; Zuo, P.; Liu, Y.; Xu, H.; Ye, B.C. Rapid on-chip isolation of cancer-associated exosomes and combined analysis of exosomes and exosomal proteins. *Anal. Chem.* **2022**, *94*, 7703–7712. [CrossRef] [PubMed]
45. Xu, H.; Liao, C.; Zuo, P.; Liu, Z.; Ye, B.C. Magnetic-based microfluidic device for on-chip isolation and detection of tumor-derived exosomes. *Anal. Chem.* **2018**, *90*, 13451–13458. [CrossRef]
46. Shen, K.-M.; Sabbavarapu, N.M.; Fu, C.-Y.; Jan, J.-T.; Wang, J.-R.; Hung, S.-C.; Lee, G.-B. An integrated microfluidic system for rapid detection and multiple subtyping of influenza A viruses by using glycan-coated magnetic beads and RT-PCR. *Lab Chip* **2019**, *19*, 1277–1286. [CrossRef]
47. Lee, M.S.; Hyun, H.; Park, I.; Kim, S.; Jang, D.H.; Kim, S.; Im, J.K.; Kim, H.; Lee, J.H.; Kwon, T.; et al. Quantitative fluorescence in situ hybridization (FISH) of magnetically confined bacteria enables early detection of human bacteremia. *Small Methods* **2022**, *6*, e2101239. [CrossRef]
48. Wang, C.H.; Chang, C.J.; Wu, J.J.; Lee, G.B. An integrated microfluidic device utilizing vancomycin conjugated magnetic beads and nanogold-labeled specific nucleotide probes for rapid pathogen diagnosis. *Nanomedicine* **2014**, *10*, 809–818. [CrossRef]
49. Xia, L.; Li, Y.; Liu, Y.; Li, G.; Xiao, X. Recent advances in sample preparation techniques in China. *J. Sep. Sci.* **2020**, *43*, 189–201. [CrossRef]
50. Schneider, L.; Usherwood, T.; Tripathi, A. A microfluidic platform for high-purity cell free DNA extraction from plasma for non-invasive prenatal testing. *Prenat. Diagn.* **2022**, *42*, 240–253. [CrossRef]
51. Shamloo, A.; Selahi, A.; Madadelahi, M. Designing and modeling a centrifugal microfluidic device to separate target blood cells. *J. Micromech. Microeng.* **2016**, *26*, 035017. [CrossRef]
52. Xue, M.; Xiang, A.; Guo, Y.; Wang, L.; Wang, R.; Wang, W.; Ji, G.; Lu, Z. Dynamic Halbach array magnet integrated microfluidic system for the continuous-flow separation of rare tumor cells. *RSC Adv.* **2019**, *9*, 38496–38504. [CrossRef]
53. Zirath, H.; Peham, J.R.; Schnetz, G.; Coll, A.; Brandhoff, L.; Spittler, A.; Vellekoop, M.J.; Redl, H. A compact and integrated immunoassay with on-chip dispensing and magnetic particle handling. *Biomed. Microdevices* **2016**, *18*, 16. [CrossRef]
54. Loo, J.F.; Lau, P.M.; Kong, S.K.; Ho, H.P. An assay using localized surface plasmon resonance and gold nanorods functionalized with aptamers to sense the cytochrome-c released from apoptotic cancer cells for anti-cancer drug effect determination. *Micromachines* **2017**, *8*, 338. [CrossRef]
55. Vaculovicova, M.; Smerkova, K.; Sedlacek, J.; Vyslouzil, J.; Hubalek, J.; Kizek, R.; Adam, V. Integrated chip electrophoresis and magnetic particle isolation used for detection of hepatitis B virus oligonucleotides. *Electrophoresis* **2013**, *34*, 1548–1554. [CrossRef]
56. Chen, K.C.; Pan, Y.C.; Chen, C.L.; Lin, C.H.; Huang, C.S.; Wo, A.M. Enumeration and viability of rare cells in a microfluidic disk via positive selection approach. *Anal. Biochem.* **2012**, *429*, 116–123. [CrossRef]
57. Tang, M.; Wen, C.Y.; Wu, L.L.; Hong, S.L.; Hu, J.; Xu, C.M.; Pang, D.W.; Zhang, Z.L. A chip assisted immunomagnetic separation system for the efficient capture and in situ identification of circulating tumor cells. *Lab Chip* **2016**, *16*, 1214–1223. [CrossRef]
58. Wang, Z.; Sargent, E.H.; Kelley, S.O. Ultrasensitive detection and depletion of rare leukemic B cells in T cell populations via immunomagnetic cell ranking. *Anal. Chem.* **2021**, *93*, 2327–2335. [CrossRef]
59. Kongsuphol, P.; Liu, Y.; Ramadan, Q. On-chip immune cell activation and subsequent time-resolved magnetic bead-based cytokine detection. *Biomed. Microdevices* **2016**, *18*, 93. [CrossRef]
60. Hong, S.-L.; Yu, Z.-L.; Bao, Z.-H.; Zhang, Q.-Y.; Zhang, N.; Tang, M.; Liu, S.-Q.; Jia, J.; Liu, K. One-step detection of oral ulcers and oral cancer derived exosomes on wedge-shaped and high magnetic field gradient mediated chip. *Sens. Actuators B Chem.* **2022**, *357*, 131403. [CrossRef]
61. Chao, C.Y.; Wang, C.H.; Che, Y.J.; Kao, C.Y.; Wu, J.J.; Lee, G.B. An integrated microfluidic system for diagnosis of the resistance of *Helicobacter pylori* to quinolone-based antibiotics. *Biosens. Bioelectron.* **2016**, *78*, 281–289. [CrossRef]
62. Cheng, Y.H.; Wang, C.H.; Hsu, K.F.; Lee, G.B. Integrated microfluidic system for cell-free DNA extraction from plasma for mutant gene detection and quantification. *Anal. Chem.* **2022**, *94*, 4311–4318. [CrossRef] [PubMed]
63. Wang, C.-H.; Lien, K.-Y.; Hung, L.-Y.; Lei, H.-Y.; Lee, G.-B. Integrated microfluidic system for the identification and multiple subtyping of influenza viruses by using a molecular diagnostic approach. *Microfluid. Nanofluidics* **2012**, *13*, 113–123. [CrossRef]
64. Castro-Lopez, V.; Elizalde, J.; Pacek, M.; Hijona, E.; Bujanda, L. A simple and portable device for the quantification of TNF-α in human plasma by means of on-chip magnetic bead-based proximity ligation assay. *Biosens. Bioelectron.* **2014**, *54*, 499–505. [CrossRef] [PubMed]
65. Zhang, R.Q.; Hong, S.L.; Wen, C.Y.; Pang, D.W.; Zhang, Z.L. Rapid detection and subtyping of multiple influenza viruses on a microfluidic chip integrated with controllable micro-magnetic field. *Biosens. Bioelectron.* **2018**, *100*, 348–354. [CrossRef]

66. Wang, S.; Ai, Z.; Zhang, Z.; Tang, M.; Zhang, N.; Liu, F.; Han, G.; Hong, S.L.; Liu, K. Simultaneous and automated detection of influenza A virus hemagglutinin H7 and H9 based on magnetism and size mediated microfluidic chip. *Sens. Actuators B Chem.* **2020**, *308*, 127675. [CrossRef]
67. Sung, C.Y.; Huang, C.C.; Chen, Y.S.; Hsu, K.F.; Lee, G.B. Isolation and quantification of extracellular vesicle-encapsulated microRNA on an integrated microfluidic platform. *Lab Chip* **2021**, *21*, 4660–4671. [CrossRef]
68. Malhotra, R.; Patel, V.; Chikkaveeraiah, B.V.; Munge, B.S.; Cheong, S.C.; Zain, R.B.; Abraham, M.T.; Dey, D.K.; Gutkind, J.S.; Rusling, J.F. Ultrasensitive detection of cancer biomarkers in the clinic by use of a nanostructured microfluidic array. *Anal. Chem.* **2012**, *84*, 6249–6255. [CrossRef]
69. Otieno, B.A.; Krause, C.E.; Latus, A.; Chikkaveeraiah, B.V.; Faria, R.C.; Rusling, J.F. On-line protein capture on magnetic beads for ultrasensitive microfluidic immunoassays of cancer biomarkers. *Biosens. Bioelectron.* **2014**, *53*, 268–274. [CrossRef]
70. Otieno, B.A.; Krause, C.E.; Jones, A.L.; Kremer, R.B.; Rusling, J.F. Cancer diagnostics via ultrasensitive multiplexed detection of parathyroid hormone-related peptides with a microfluidic immunoarray. *Anal. Chem.* **2016**, *88*, 9269–9275. [CrossRef]
71. De Oliveira, R.A.G.; Nicoliche, C.Y.N.; Pasqualeti, A.M.; Shimizu, F.M.; Ribeiro, I.R.; Melendez, M.E.; Carvalho, A.L.; Gobbi, A.L.; Faria, R.C.; Lima, R.S. Low-cost and rapid-production microfluidic electrochemical double-layer capacitors for fast and sensitive breast cancer diagnosis. *Anal. Chem.* **2018**, *90*, 12377–12384. [CrossRef]
72. Moral-Vico, J.; Barallat, J.; Abad, L.; Olive-Monllau, R.; Munoz-Pascual, F.X.; Galan Ortega, A.; del Campo, F.J.; Baldrich, E. Dual chronoamperometric detection of enzymatic biomarkers using magnetic beads and a low-cost flow cell. *Biosens. Bioelectron.* **2015**, *69*, 328–336. [CrossRef]
73. Raj, N.; Crooks, R.M. Plastic-based lateral flow immunoassay device for electrochemical detection of NT-proBNP. *Analyst* **2022**, *147*, 2460–2469. [CrossRef]
74. Zirath, H.; Schnetz, G.; Glatz, A.; Spittler, A.; Redl, H.; Peham, J.R. Bedside immune monitoring: An automated immunoassay platform for quantification of blood biomarkers in patient serum within 20 minutes. *Anal. Chem.* **2017**, *89*, 4817–4823. [CrossRef]
75. Yang, R.; Li, F.; Zhang, W.; Shen, W.; Yang, D.; Bian, Z.; Cui, H. Chemiluminescence immunoassays for simultaneous detection of three heart disease biomarkers using magnetic carbon composites and three-dimensional microfluidic paper-based device. *Anal. Chem.* **2019**, *91*, 13006–13013. [CrossRef]
76. Gao, R.; Lv, Z.; Mao, Y.; Yu, L.; Bi, X.; Xu, S.; Cui, J.; Wu, Y. SERS-based pump-free microfluidic chip for highly sensitive immunoassay of prostate-specific antigen biomarkers. *ACS Sens.* **2019**, *4*, 938–943. [CrossRef]
77. Gao, R.; Cheng, Z.; Wang, X.; Yu, L.; Guo, Z.; Zhao, G.; Choo, J. Simultaneous immunoassays of dual prostate cancer markers using a SERS-based microdroplet channel. *Biosens. Bioelectron.* **2018**, *119*, 126–133. [CrossRef]
78. Gasilova, N.; Qiao, L.; Momotenko, D.; Pourhaghighi, M.R.; Girault, H.H. Microchip emitter for solid-phase extraction-gradient elution-mass spectrometry. *Anal. Chem.* **2013**, *85*, 6254–6263. [CrossRef]
79. Gasilova, N.; Srzentic, K.; Qiao, L.; Liu, B.; Beck, A.; Tsybin, Y.O.; Girault, H.H. On-chip mesoporous functionalized magnetic microspheres for protein sequencing by extended bottom-up mass spectrometry. *Anal. Chem.* **2016**, *88*, 1775–1784. [CrossRef]
80. Zitka, O.; Cernei, N.; Heger, Z.; Matousek, M.; Kopel, P.; Kynicky, J.; Masarik, M.; Kizek, R.; Adam, V. Microfluidic chip coupled with modified paramagnetic particles for sarcosine isolation in urine. *Electrophoresis* **2013**, *34*, 2639–2647. [CrossRef]
81. Liang, R.P.; Liu, C.M.; Meng, X.Y.; Wang, J.W.; Qiu, J.D. A novel open-tubular capillary electrochromatography using β-cyclodextrin functionalized graphene oxide-magnetic nanocomposites as tunable stationary phase. *J. Chromatogr. A* **2012**, *1266*, 95–102. [CrossRef] [PubMed]
82. Piao, J.; Liu, L.; Cai, L.; Ri, H.C.; Jin, X.; Sun, H.; Piao, X.; Shang, H.B.; Jin, X.; Pu, Q.; et al. High-resolution micro-object separation by rotating magnetic chromatography. *Anal. Chem.* **2022**, *94*, 11500–11507. [CrossRef] [PubMed]
83. Shim, S.; Shim, J.; Taylor, W.R.; Kosari, F.; Vasmatzis, G.; Ahlquist, D.A.; Bashir, R. Magnetophoretic-based microfluidic device for DNA concentration. *Biomed. Microdevices* **2016**, *18*, 28. [CrossRef] [PubMed]
84. Tian, M.; Feng, W.; Ye, J.; Jia, Q. Preparation of Fe_3O_4@TiO_2/graphene oxide magnetic microspheres for microchip-based preconcentration of estrogens in milk and milk powder samples. *Anal. Methods* **2013**, *5*, 3984. [CrossRef]
85. Lee, T.Y.; Hyun, K.-A.; Kim, S.-I.; Jung, H.-I. An integrated microfluidic chip for one-step isolation of circulating tumor cells. *Sens. Actuators B Chem.* **2017**, *238*, 1144–1150. [CrossRef]
86. Abafogi, A.T.; Kim, J.; Lee, J.; Mohammed, M.O.; van Noort, D.; Park, S. 3D-printed modular microfluidic device enabling preconcentrating bacteria and purifying bacterial DNA in blood for improving the sensitivity of molecular diagnostics. *Sensors* **2020**, *20*, 1202. [CrossRef]
87. De Oliveira, R.A.G.; Materon, E.M.; Melendez, M.E.; Carvalho, A.L.; Faria, R.C. Disposable microfluidic immunoarray device for sensitive breast cancer biomarker detection. *ACS Appl. Mater. Interfaces* **2017**, *9*, 27433–27440. [CrossRef]
88. Mou, L.; Hong, H.; Xu, X.; Xia, Y.; Jiang, X. Digital hybridization human papillomavirus assay with attomolar sensitivity without amplification. *ACS Nano* **2021**, *15*, 13077–13084. [CrossRef]
89. Zhang, H.; Yi, Y.; Zhou, C.; Ying, G.; Zhou, X.; Fu, C.; Zhu, Y.; Shen, Y. SERS detection of microRNA biomarkers for cancer diagnosis using gold-coated paramagnetic nanoparticles to capture SERS-active gold nanoparticles. *RSC Adv.* **2017**, *7*, 52782–52793. [CrossRef]
90. Mousavi, M.Z.; Chen, H.Y.; Wu, S.H.; Peng, S.W.; Lee, K.L.; Wei, P.K.; Cheng, J.Y. Magnetic nanoparticle-enhanced SPR on gold nanoslits for ultra-sensitive, label-free detection of nucleic acid biomarkers. *Analyst* **2013**, *138*, 2740–2748. [CrossRef]

91. Wang, Y.; Ye, Z.; Ping, J.; Jing, S.; Ying, Y. Development of an aptamer-based impedimetric bioassay using microfluidic system and magnetic separation for protein detection. *Biosens. Bioelectron.* **2014**, *59*, 106–111. [CrossRef]
92. Sheng, J.; Zhang, L.; Lei, J.; Ju, H. Fabrication of tunable microreactor with enzyme modified magnetic nanoparticles for microfluidic electrochemical detection of glucose. *Anal. Chim. Acta.* **2012**, *709*, 41–46. [CrossRef]
93. Mohamadi, R.M.; Svobodova, Z.; Bilkova, Z.; Otto, M.; Taverna, M.; Descroix, S.; Viovy, J.L. An integrated microfluidic chip for immunocapture, preconcentration and separation of β-amyloid peptides. *Biomicrofluidics* **2015**, *9*, 054117. [CrossRef]
94. Tsai, H.Y.; Wu, H.H.; Chou, B.C.; Li, C.S.; Gau, B.Z.; Lin, Z.Y.; Fuh, C.B. A magneto-microfluidic platform for fluorescence immunosensing using quantum dot nanoparticles. *Nanotechnology* **2019**, *30*, 505101. [CrossRef]
95. Liu, W.; Zhou, X.; Xing, D. Rapid and reliable microRNA detection by stacking hybridization on electrochemiluminescent chip system. *Biosens. Bioelectron.* **2014**, *58*, 388–394. [CrossRef]
96. Proenca, C.A.; Freitas, T.A.; Baldo, T.A.; Materon, E.M.; Shimizu, F.M.; Ferreira, G.R.; Soares, F.L.F.; Faria, R.C.; Oliveira, O.N., Jr. Use of data processing for rapid detection of the prostate-specific antigen biomarker using immunomagnetic sandwich-type sensors. *Beilstein J. Nanotechnol.* **2019**, *10*, 2171–2181. [CrossRef]
97. Ma, Y.-D.; Chen, Y.-S.; Lee, G.-B. An integrated self-driven microfluidic device for rapid detection of the influenza A (H1N1) virus by reverse transcription loop-mediated isothermal amplification. *Sens. Actuators B Chem.* **2019**, *296*, 126647. [CrossRef]
98. Zhao, Z.; Bao, Y.; Chu, L.T.; Ho, J.K.L.; Chieng, C.C.; Chen, T.H. Microfluidic bead trap as a visual bar for quantitative detection of oligonucleotides. *Lab Chip* **2017**, *17*, 3240–3245. [CrossRef]
99. Huang, R.; Quan, J.; Su, B.; Cai, C.; Cai, S.; Chen, Y.; Mou, Z.; Zhou, P.; Ma, D.; Cui, X. A two-step competition assay for visual, sensitive and quantitative C-reactive protein detection in low-cost microfluidic particle accumulators. *Sens. Actuators B Chem.* **2022**, *359*, 131583. [CrossRef]
100. Liang, W.; Li, Y.; Zhang, B.; Zhang, Z.; Chen, A.; Qi, D.; Yi, W.; Hu, C. A novel microfluidic immunoassay system based on electrochemical immunosensors: An application for the detection of NT-proBNP in whole blood. *Biosens. Bioelectron.* **2012**, *31*, 480–485. [CrossRef]
101. Huang, J.; Huang, C.; Zhong, W.; Lin, Y. A magneto-controlled microfluidic device for voltammetric immunoassay of carbohydrate antigen-125 with silver–polypyrrole nanotags. *Anal. Methods* **2020**, *12*, 4211–4219. [CrossRef]
102. Liu, G.; Cao, C.; Ni, S.; Feng, S.; Wei, H. On-chip structure-switching aptamer-modified magnetic nanobeads for the continuous monitoring of interferon-gamma ex vivo. *Microsyst. Nanoeng.* **2019**, *5*, 35. [CrossRef] [PubMed]
103. Lin, Y.H.; Wang, S.H.; Wu, M.H.; Pan, T.M.; Lai, C.S.; Luo, J.D.; Chiou, C.C. Integrating solid-state sensor and microfluidic devices for glucose, urea and creatinine detection based on enzyme-carrying alginate microbeads. *Biosens. Bioelectron.* **2013**, *43*, 328–335. [CrossRef] [PubMed]
104. Mercer, C.; Jones, A.; Rusling, J.F.; Leech, D. Multiplexed electrochemical cancer diagnostics with automated microfluidics. *Electroanalysis* **2019**, *31*, 208–211. [CrossRef] [PubMed]
105. Li, J.; Lillehoj, P.B. Microfluidic magneto immunosensor for rapid, high sensitivity measurements of SARS-CoV-2 nucleocapsid protein in serum. *ACS Sens.* **2021**, *6*, 1270–1278. [CrossRef]
106. Ruiz-Vega, G.; Arias-Alpizar, K.; de la Serna, E.; Borgheti-Cardoso, L.N.; Sulleiro, E.; Molina, I.; Fernandez-Busquets, X.; Sanchez-Montalva, A.; Del Campo, F.J.; Baldrich, E. Electrochemical POC device for fast malaria quantitative diagnosis in whole blood by using magnetic beads, Poly-HRP and microfluidic paper electrodes. *Biosens. Bioelectron.* **2020**, *150*, 111925. [CrossRef]
107. Chen, W.L.; Jayan, M.; Kwon, J.S.; Chuang, H.S. Facile open-well immunofluorescence enhancement with coplanar-electrodes-enabled optoelectrokinetics and magnetic particles. *Biosens. Bioelectron.* **2021**, *193*, 113527. [CrossRef]
108. Hung, L.Y.; Huang, T.B.; Tsai, Y.C.; Yeh, C.S.; Lei, H.Y.; Lee, G.B. A microfluidic immunomagnetic bead-based system for the rapid detection of influenza infections: From purified virus particles to clinical specimens. *Biomed. Microdevices* **2013**, *15*, 539–551. [CrossRef]
109. Huang, W.; Chang, C.L.; Chan, B.D.; Jalal, S.I.; Matei, D.E.; Low, P.S.; Savran, C.A. Concurrent detection of cellular and molecular cancer markers using an immunomagnetic flow system. *Anal. Chem.* **2015**, *87*, 10205–10212. [CrossRef]
110. Yang, J.; Xiao, X.; Xia, L.; Li, G.; Shui, L. Microfluidic magnetic analyte delivery technique for separation, enrichment, and fluorescence detection of ultratrace biomarkers. *Anal. Chem.* **2021**, *93*, 8273–8280. [CrossRef]
111. Dong, J.; Li, G.; Xia, L. Microfluidic magnetic spatial confinement strategy for the enrichment and ultrasensitive detection of MCF-7 and *Escherichia coli* O157:H7. *Anal. Chem.* **2022**, *94*, 16901–16909. [CrossRef]
112. Arias-Alpizar, K.; Sanchez-Cano, A.; Prat-Trunas, J.; de la Serna Serna, E.; Alonso, O.; Sulleiro, E.; Sanchez-Montalva, A.; Dieguez, A.; Baldrich, E. Malaria quantitative POC testing using magnetic particles, a paper microfluidic device and a hand-held fluorescence reader. *Biosens. Bioelectron.* **2022**, *215*, 114513. [CrossRef]
113. Gao, R.; Ko, J.; Cha, K.; Jeon, J.H.; Rhie, G.E.; Choi, J.; deMello, A.J.; Choo, J. Fast and sensitive detection of an anthrax biomarker using SERS-based solenoid microfluidic sensor. *Biosens. Bioelectron.* **2015**, *72*, 230–236. [CrossRef]
114. Li, J.; Skeete, Z.; Shan, S.; Yan, S.; Kurzatkowska, K.; Zhao, W.; Ngo, Q.M.; Holubovska, P.; Luo, J.; Hepel, M.; et al. Surface enhanced Raman scattering detection of cancer biomarkers with bifunctional nanocomposite probes. *Anal. Chem.* **2015**, *87*, 10698–10702. [CrossRef]
115. Wang, Y.; Li, Q.; Shi, H.; Tang, K.; Qiao, L.; Yu, G.; Ding, C.; Yu, S. Microfluidic Raman biochip detection of exosomes: A promising tool for prostate cancer diagnosis. *Lab Chip* **2020**, *20*, 4632–4637. [CrossRef]

116. Wen, X.; Ou, Y.C.; Zarick, H.F.; Zhang, X.; Hmelo, A.B.; Victor, Q.J.; Paul, E.P.; Slocik, J.M.; Naik, R.R.; Bellan, L.M.; et al. PRADA: Portable Reusable Accurate Diagnostics with nanostar Antennas for multiplexed biomarker screening. *Bioeng. Transl. Med.* **2020**, *5*, e10165. [CrossRef]
117. Ge, S.; Li, G.; Zhou, X.; Mao, Y.; Gu, Y.; Li, Z.; Gu, Y.; Cao, X. Pump-free microfluidic chip based laryngeal squamous cell carcinoma-related microRNAs detection through the combination of surface-enhanced Raman scattering techniques and catalytic hairpin assembly amplification. *Talanta* **2022**, *245*, 123478. [CrossRef]
118. Cao, X.; Ge, S.; Zhou, X.; Mao, Y.; Sun, Y.; Lu, W.; Ran, M. A dual-signal amplification strategy based on pump-free SERS microfluidic chip for rapid and ultrasensitive detection of non-small cell lung cancer-related circulating tumour DNA in mice serum. *Biosens. Bioelectron.* **2022**, *205*, 114110. [CrossRef]
119. Park, S.; Su Jeon, C.; Choi, N.; Moon, J.I.; Min Lee, K.; Hyun Pyun, S.; Kang, T.; Choo, J. Sensitive and reproducible detection of SARS-CoV-2 using SERS-based microdroplet sensor. *Chem. Eng. J.* **2022**, *446*, 137085. [CrossRef]
120. Guo, X. Fe_3O_4@Au nanoparticles enhanced surface plasmon resonance for ultrasensitive immunoassay. *Sens. Actuators B Chem.* **2014**, *205*, 276–280. [CrossRef]
121. Bigdeli, Y.; Preetam, S.; Scott, K.C.; Zhong, Z.; Liang, T.-C.; Chakrabarty, K.; Fair, R.B.; Gray, B.L.; Becker, H. Fluorescent detection of nucleosomes using functionalized magnetic beads on a digital microfluidic device. In Proceedings of the Microfluidics, BioMEMS, and Medical Microsystems XIX, Online, 6–11 March 2021; p. 116370L.
122. Shamsi, M.H.; Choi, K.; Ng, A.H.; Wheeler, A.R. A digital microfluidic electrochemical immunoassay. *Lab Chip* **2014**, *14*, 547–554. [CrossRef] [PubMed]
123. Metzler, L.; Rehbein, U.; Schonberg, J.N.; Brandstetter, T.; Thedieck, K.; Ruhe, J. Breaking the interface: Efficient extraction of magnetic beads from nanoliter droplets for automated sequential immunoassays. *Anal. Chem.* **2020**, *92*, 10283–10290. [CrossRef] [PubMed]
124. Lin, T.T.; Wang, J.W.; Shi, Q.N.; Wang, H.F.; Pan, J.Z.; Fang, Q. An automated, fully-integrated nucleic acid analyzer based on microfluidic liquid handling robot technique. *Anal. Chim. Acta* **2023**, *1239*, 340698. [CrossRef] [PubMed]
125. Zhou, W. Development of immunomagnetic droplet-based digital immuno-PCR for the quantification of prostate specific antigen. *Anal. Methods* **2018**, *10*, 3690–3695. [CrossRef]
126. Kim, J.A.; Kim, M.; Kang, S.M.; Lim, K.T.; Kim, T.S.; Kang, J.Y. Magnetic bead droplet immunoassay of oligomer amyloid β for the diagnosis of Alzheimer's disease using micro-pillars to enhance the stability of the oil-water interface. *Biosens. Bioelectron.* **2015**, *67*, 724–732. [CrossRef]
127. Huang, E.; Huang, D.; Wang, Y.; Cai, D.; Luo, Y.; Zhong, Z.; Liu, D. Active droplet-array microfluidics-based chemiluminescence immunoassay for point-of-care detection of procalcitonin. *Biosens. Bioelectron.* **2022**, *195*, 113684. [CrossRef]
128. Lu, P.H.; Ma, Y.D.; Fu, C.Y.; Lee, G.B. A structure-free digital microfluidic platform for detection of influenza a virus by using magnetic beads and electromagnetic forces. *Lab Chip* **2020**, *20*, 789–797. [CrossRef]
129. Kuhnemund, M.; Witters, D.; Nilsson, M.; Lammertyn, J. Circle-to-circle amplification on a digital microfluidic chip for amplified single molecule detection. *Lab Chip* **2014**, *14*, 2983–2992. [CrossRef]
130. Okochi, M.; Koike, S.; Tanaka, M.; Honda, H. Detection of *Her2*-overexpressing cancer cells using keyhole shaped chamber array employing a magnetic droplet-handling system. *Biosens. Bioelectron.* **2017**, *93*, 32–39. [CrossRef]
131. Gaddes, D.E.; Lee, P.W.; Trick, A.Y.; Athamanolap, P.; O'Keefe, C.M.; Puleo, C.; Hsieh, K.; Wang, T.H. Facile coupling of droplet magnetofluidic-enabled automated sample preparation for digital nucleic acid amplification testing and analysis. *Anal. Chem.* **2020**, *92*, 13254–13261. [CrossRef]
132. Phurimsak, C.; Tarn, M.D.; Peyman, S.A.; Greenman, J.; Pamme, N. On-chip determination of C-reactive protein using magnetic particles in continuous flow. *Anal. Chem.* **2014**, *86*, 10552–10559. [CrossRef]
133. Xiong, Q.; Lim, C.Y.; Ren, J.; Zhou, J.; Pu, K.; Chan-Park, M.B.; Mao, H.; Lam, Y.C.; Duan, H. Magnetic nanochain integrated microfluidic biochips. *Nat. Commun.* **2018**, *9*, 1743. [CrossRef]
134. Seder, I.; Kim, D.-M.; Hwang, S.-H.; Sung, H.; Kim, D.-E.; Kim, S.-J. Fluidic handling system for PCR-based sample-to-answer detection of viral nucleic acids. *Sens. Actuators B Chem.* **2021**, *349*, 130788. [CrossRef]
135. Turiello, R.; Dignan, L.M.; Thompson, B.; Poulter, M.; Hickey, J.; Chapman, J.; Landers, J.P. Centrifugal microfluidic method for enrichment and enzymatic extraction of severe acute respiratory syndrome coronavirus 2 RNA. *Anal. Chem.* **2022**, *94*, 3287–3295. [CrossRef]
136. Seder, I.; Jo, A.; Jun, B.H.; Kim, S.J. Movable layer device for rapid detection of influenza a H1N1 virus using highly bright multi-quantum dot-embedded particles and magnetic beads. *Nanomaterials* **2022**, *12*, 284. [CrossRef]
137. Kabir, M.A.; Zilouchian, H.; Sher, M.; Asghar, W. Development of a flow-free automated colorimetric detection assay integrated with smartphone for Zika NS1. *Diagnostics* **2020**, *10*, 42. [CrossRef]
138. Garbarino, F.; Minero, G.A.S.; Rizzi, G.; Fock, J.; Hansen, M.F. Integration of rolling circle amplification and optomagnetic detection on a polymer chip. *Biosens. Bioelectron.* **2019**, *142*, 111485. [CrossRef]
139. Czilwik, G.; Vashist, S.K.; Klein, V.; Buderer, A.; Roth, G.; von Stetten, F.; Zengerle, R.; Mark, D. Magnetic chemiluminescent immunoassay for human C-reactive protein on the centrifugal microfluidics platform. *RSC Adv.* **2015**, *5*, 61906–61912. [CrossRef]
140. Yang, Y.; Zeng, Y. Microfluidic communicating vessel chip for expedited and automated immunomagnetic assays. *Lab Chip* **2018**, *18*, 3830–3839. [CrossRef]

141. Sasso, L.A.; Johnston, I.H.; Zheng, M.; Gupte, R.K.; Undar, A.; Zahn, J.D. Automated microfluidic processing platform for multiplexed magnetic bead immunoassays. *Microfluid. Nanofluidics* **2012**, *13*, 603–612. [CrossRef]
142. Lin, Y.H.; Wu, C.C.; Peng, Y.S.; Wu, C.W.; Chang, Y.T.; Chang, K.P. Detection of anti-p53 autoantibodies in saliva using microfluidic chips for the rapid screening of oral cancer. *RSC Adv.* **2018**, *8*, 15513–15521. [CrossRef] [PubMed]
143. Zhang, L.; Deraney, R.N.; Tripathi, A. Adsorption and isolation of nucleic acids on cellulose magnetic beads using a three-dimensional printed microfluidic chip. *Biomicrofluidics* **2015**, *9*, 064118. [CrossRef] [PubMed]
144. Jalal, U.M.; Jin, G.J.; Eom, K.S.; Kim, M.H.; Shim, J.S. On-chip signal amplification of magnetic bead-based immunoassay by aviating magnetic bead chains. *Bioelectrochemistry* **2018**, *122*, 221–226. [CrossRef] [PubMed]
145. Liu, D.; Zhang, Y.; Zhu, M.; Yu, Z.; Ma, X.; Song, Y.; Zhou, S.; Yang, C. Microfluidic-integrated multicolor immunosensor for visual detection of HIV-1 p24 antigen with the naked eye. *Anal. Chem.* **2020**, *92*, 11826–11833. [CrossRef]
146. Liu, D.; Li, X.; Zhou, J.; Liu, S.; Tian, T.; Song, Y.; Zhu, Z.; Zhou, L.; Ji, T.; Yang, C. A fully integrated distance readout ELISA-Chip for point-of-care testing with sample-in-answer-out capability. *Biosens. Bioelectron.* **2017**, *96*, 332–338. [CrossRef]
147. Tekin, H.C.; Cornaglia, M.; Gijs, M.A. Attomolar protein detection using a magnetic bead surface coverage assay. *Lab Chip* **2013**, *13*, 1053–1059. [CrossRef]
148. Adel Ahmed, H.; Azzazy, H.M. Power-free chip enzyme immunoassay for detection of prostate specific antigen (PSA) in serum. *Biosens. Bioelectron.* **2013**, *49*, 478–484. [CrossRef]
149. Song, Y.; Lin, B.; Tian, T.; Xu, X.; Wang, W.; Ruan, Q.; Guo, J.; Zhu, Z.; Yang, C. Recent progress in microfluidics-based biosensing. *Anal. Chem.* **2019**, *91*, 388–404. [CrossRef]
150. Huo, W.; Gao, Y.; Zhang, L.; Shi, S.; Gao, Y. A novel high-sensitivity cardiac multibiomarker detection system based on microfluidic chip and GMR sensors. *IEEE Trans. Magn.* **2015**, *51*, 1–4. [CrossRef]
151. Zhi, X.; Liu, Q.; Zhang, X.; Zhang, Y.; Feng, J.; Cui, D. Quick genotyping detection of HBV by giant magnetoresistive biochip combined with PCR and line probe assay. *Lab Chip* **2012**, *12*, 741–745. [CrossRef]
152. Zhi, X.; Deng, M.; Yang, H.; Gao, G.; Wang, K.; Fu, H.; Zhang, Y.; Chen, D.; Cui, D. A novel HBV genotypes detecting system combined with microfluidic chip, loop-mediated isothermal amplification and GMR sensors. *Biosens. Bioelectron.* **2014**, *54*, 372–377. [CrossRef]
153. Krishna, V.D.; Wu, K.; Perez, A.M.; Wang, J.P. Giant magnetoresistance-based biosensor for detection of influenza A virus. *Front. Microbiol.* **2016**, *7*, 400. [CrossRef]
154. Wu, K.; Klein, T.; Krishna, V.D.; Su, D.; Perez, A.M.; Wang, J.P. Portable GMR handheld platform for the detection of influenza A virus. *ACS Sens.* **2017**, *2*, 1594–1601. [CrossRef]
155. Su, D.; Wu, K.; Krishna, V.D.; Klein, T.; Liu, J.; Feng, Y.; Perez, A.M.; Cheeran, M.C.; Wang, J.P. Detection of influenza A virus in swine nasal swab samples with a wash-free magnetic bioassay and a handheld giant magnetoresistance sensing system. *Front. Microbiol.* **2019**, *10*, 1077. [CrossRef]
156. Prabowo, B.A.; Fernandes, E.; Freitas, P. A pump-free microfluidic device for fast magnetic labeling of ischemic stroke biomarkers. *Anal. Bioanal. Chem.* **2022**, *414*, 2571–2583. [CrossRef]
157. Gao, Y.; Huo, W.; Zhang, L.; Lian, J.; Tao, W.; Song, C.; Tang, J.; Shi, S.; Gao, Y. Multiplex measurement of twelve tumor markers using a GMR multi-biomarker immunoassay biosensor. *Biosens. Bioelectron.* **2019**, *123*, 204–210. [CrossRef]
158. Jin, Z.; Wang, Y.; Fujiwara, K.; Oogane, M.; Ando, Y. Detection of small magnetic fields using serial magnetic tunnel junctions with various geometrical characteristics. *Sensors* **2020**, *20*, 5704. [CrossRef]
159. Sharma, P.P.; Albisetti, E.; Massetti, M.; Scolari, M.; La Torre, C.; Monticelli, M.; Leone, M.; Damin, F.; Gervasoni, G.; Ferrari, G.; et al. Integrated platform for detecting pathogenic DNA via magnetic tunneling junction-based biosensors. *Sens. Actuators B Chem.* **2017**, *242*, 280–287. [CrossRef]
160. Yin, B.; Qian, C.; Wang, S.; Wan, X.; Zhou, T. A microfluidic chip-based MRS immunosensor for biomarker detection via enzyme-mediated nanoparticle assembly. *Front. Chem.* **2021**, *9*, 688442. [CrossRef]
161. Osterberg, F.W.; Rizzi, G.; Donolato, M.; Bejhed, R.S.; Mezger, A.; Stromberg, M.; Nilsson, M.; Stromme, M.; Svedlindh, P.; Hansen, M.F. On-chip detection of rolling circle amplified DNA molecules from *Bacillus globigii* spores and *Vibrio cholerae*. *Small* **2014**, *10*, 2877–2882. [CrossRef]
162. Sharafeldin, M.; Bishop, G.W.; Bhakta, S.; El-Sawy, A.; Suib, S.L.; Rusling, J.F. Fe_3O_4 nanoparticles on graphene oxide sheets for isolation and ultrasensitive amperometric detection of cancer biomarker proteins. *Biosens. Bioelectron.* **2017**, *91*, 359–366. [CrossRef] [PubMed]
163. Feng, Z.; Zhi, S.; Guo, L.; Zhou, Y.; Lei, C. An integrated magnetic microfluidic chip for rapid immunodetection of the prostate specific antigen using immunomagnetic beads. *Mikrochim. Acta* **2019**, *186*, 252. [CrossRef] [PubMed]
164. Khodayari Bavil, A.; Sticker, D.; Rothbauer, M.; Ertl, P.; Kim, J. A microfluidic microparticle-labeled impedance sensor array for enhancing immunoassay sensitivity. *Analyst* **2021**, *146*, 3289–3298. [CrossRef] [PubMed]
165. Sayad, A.; Uddin, S.M.; Yao, S.; Wilson, H.; Chan, J.; Zhao, H.; Donnan, G.; Davis, S.; Skafidas, E.; Yan, B.; et al. A magnetoimpedance biosensor microfluidic platform for detection of glial fibrillary acidic protein in blood for acute stroke classification. *Biosens. Bioelectron.* **2022**, *211*, 114410. [CrossRef]
166. Jamshaid, T.; Neto, E.T.T.; Eissa, M.M.; Zine, N.; Kunita, M.H.; El-Salhi, A.E.; Elaissari, A. Magnetic particles: From preparation to lab-on-a-chip, biosensors, microsystems and microfluidics applications. *Trends Analyt. Chem.* **2016**, *79*, 344–362. [CrossRef]

167. Lu, R.; Lei, P.; Yang, Q.; Ni, Z.; Yi, H. Development of a microfluidic NMR device for rapid and quantitative detection of tumor markers. *Appl. Magn. Reson.* **2018**, *50*, 357–370. [CrossRef]
168. Donolato, M.; Antunes, P.; de la Torre, T.Z.; Hwu, E.T.; Chen, C.H.; Burger, R.; Rizzi, G.; Bosco, F.G.; Stromme, M.; Boisen, A.; et al. Quantification of rolling circle amplified DNA using magnetic nanobeads and a Blu-ray optical pick-up unit. *Biosens. Bioelectron.* **2015**, *67*, 649–655. [CrossRef]
169. Uddin, R.; Donolato, M.; Hwu, E.-T.; Hansen, M.F.; Boisen, A. Combined detection of C-reactive protein and PBMC quantification from whole blood in an integrated lab-on-a-disc microfluidic platform. *Sens. Actuators B Chem.* **2018**, *272*, 634–642. [CrossRef]
170. DuVall, J.A.; Cabaniss, S.T.; Angotti, M.L.; Moore, J.H.; Abhyankar, M.; Shukla, N.; Mills, D.L.; Kessel, B.G.; Garner, G.T.; Swami, N.S.; et al. Rapid detection of *Clostridium difficile* via magnetic bead aggregation in cost-effective polyester microdevices with cell phone image analysis. *Analyst* **2016**, *141*, 5637–5645. [CrossRef]
171. Ouyang, Y.; Li, J.; Haverstick, D.M.; Landers, J.P. Rotation-driven microfluidic disc for white blood cell enumeration using magnetic bead aggregation. *Anal. Chem.* **2016**, *88*, 11046–11054. [CrossRef]
172. Kim, S.; Han, S.; Lee, J. Asymmetric bead aggregation for microfluidic immunodetection. *Lab Chip* **2017**, *17*, 2095–2103. [CrossRef]
173. Li, H.; Huo, W.; He, M.; Lian, J.; Zhang, S.; Gao, Y. On-Chip determination of glycated hemoglobin with a novel boronic acid copolymer. *Sens. Actuators B Chem.* **2017**, *253*, 542–551. [CrossRef]
174. Raja, B.; Pascente, C.; Knoop, J.; Shakarisaz, D.; Sherlock, T.; Kemper, S.; Kourentzi, K.; Renzi, R.F.; Hatch, A.V.; Olano, J.; et al. An embedded microretroreflector-based microfluidic immunoassay platform. *Lab Chip* **2016**, *16*, 1625–1635. [CrossRef]
175. Chen, H.; Chen, C.; Bai, S.; Gao, Y.; Metcalfe, G.; Cheng, W.; Zhu, Y. Multiplexed detection of cancer biomarkers using a microfluidic platform integrating single bead trapping and acoustic mixing techniques. *Nanoscale* **2018**, *10*, 20196–20206. [CrossRef]
176. Ge, C.; Feng, J.; Zhang, J.; Hu, K.; Wang, D.; Zha, L.; Hu, X.; Li, R. Aptamer/antibody sandwich method for digital detection of SARS-CoV2 nucleocapsid protein. *Talanta* **2022**, *236*, 122847. [CrossRef]
177. Liang, L.; Ge, S.; Li, L.; Liu, F.; Yu, J. Microfluidic paper-based multiplex colorimetric immunodevice based on the catalytic effect of Pd/Fe_3O_4@C peroxidase mimetics on multiple chromogenic reactions. *Anal. Chim. Acta* **2015**, *862*, 70–76. [CrossRef]
178. Proenca, C.A.; Baldo, T.A.; Freitas, T.A.; Materon, E.M.; Wong, A.; Duran, A.A.; Melendez, M.E.; Zambrano, G.; Faria, R.C. Novel enzyme-free immunomagnetic microfluidic device based on $Co_{0.25}Zn_{0.75}Fe_2O_4$ for cancer biomarker detection. *Anal. Chim. Acta* **2019**, *1071*, 59–69. [CrossRef]
179. Wilson, R.E., Jr.; O'Connor, R.; Gallops, C.E.; Kwizera, E.A.; Noroozi, B.; Morshed, B.I.; Wang, Y.; Huang, X. Immunomagnetic capture and multiplexed surface marker detection of circulating tumor cells with magnetic multicolor surface-enhanced Raman scattering nanotags. *ACS Appl. Mater. Interfaces* **2020**, *12*, 47220–47232. [CrossRef]